Granular Matter (2015) 17:49–72
DOI 10.1007/s10035-014-0536-y

ORIGINAL PAPER

Experimental study of nonlinear acoustic bands and propagating breathers in ordered granular media embedded in matrix

M. Arif Hasan · Shinhu Cho · Kevin Remick · Alexander F. Vakakis · D. Michael McFarland · Waltraud M. Kriven

Received: 2 March 2014 / Published online: 21 December 2014

Abstract We experimentally study acoustic pass and stop-bands, and propagating breathers in harmonically excited, ordered granular chains composed of steel beads embedded in three different types of matrix—namely PDMS, polyurethane and geopolymer. Both single and coupled granular chains are tested and the bands and breathers are robustly detected in each case over varying frequency and amplitude ranges. Low-frequency acoustic pass-bands are characterized by pulse-like transmission in the granular media and negligible effective compression, whereas high-frequency stop-bands are characterized exhibit complete filtering of granular media dynamics and strong effective compression. At intermediate frequency ranges we observe the propagation of propagating breathers in the granular chains, in the form of wavetrains of localized wavepackets separated by silent regions. We study the effects of the matrix and the distance between coupled granular chains on the propagation of the breathers, and confirm the robustness of these highly nonlinear responses in this highly discontinuous class of acoustic metamaterials. Moreover, we relate our results to energy transfers between coupled granular chains. Finally, we propose a simplified theoretical model that fully recovers the experimentally detected responses. To the authors' knowledge this is the first experimental report of acoustic filtering and experimental breathers in practical acoustic nonlinear metamaterials.

Keywords Acoustic granular metamaterials · Traveling breathers · Acoustic stop and pass-bands

M. A. Hasan (✉) · S. Cho · K. Remick · A. F. Vakakis
Department of Mechanical Science and Engineering, University of Illinois at Urbana – Champaign, 1206 West Green Street, Urbana, IL 61822, USA
e-mail: mhasan5@illinois.edu

S. Cho
e-mail: cho119@illinois.edu

K. Remick
e-mail: kremick74@gmail.com

A. F. Vakakis
e-mail: avakakis@illinois.edu

D. M. McFarland
Department of Aerospace Engineering, University of Illinois at Urbana – Champaign, 319L Talbot Lab, 104 S. Wright Street, Urbana, IL 61801, USA
e-mail: dmmcf@illinois.edu

W. M. Kriven
Department of Materials Science and Engineering, University of Illinois at Urbana – Champaign, 1304 W. Green St., Urbana, IL 61801, USA
e-mail: kriven@illinois.edu

1 Introduction

Passive control of energy flow by means of trapping, redirection and scattering has been the subject of considerable attention in recent years. The use of ordered granular media is a promising candidate for such designs [8]. Ordered granular media are a type of ordered aggregates, where the neighboring particles (or granules) interact elastically in a highly nonlinear fashion. These highly discontinuous media have strongly nonlinear behavior owing to Hertzian interactions between granules in compression and separations—collisions of the same granules in the absence of compression [32]. In ordered uncompressed granular media, it is possible for neighboring beads to separate (due to loss of contact) in the absence of compressive forces. Then the dynamics become non-smooth as beads regain contact through isolated or repetitive collisions. Moreover, due to their essential (non-linearizable) nonlinearities, the acoustics of these media is highly adaptive to different applied excitations and

static preloading [9,32]. In an acoustic analogy, they can be viewed as "sonic vacua" [31]—media with zero speed of sound as defined by the classical wave equation. This is due to the nonlinearizable nature of the Hertzian interactions between granules, rendering the resulting acoustics also nonlinearizable and, hence, essentially nonlinear. Due to their strongly nonlinear acoustics uncompressed ordered granular media possess very rich dynamics, such as solitary waves [7,25,27,33], traveling waves [36], nonlinear normal modes [23], and propagating and standing breathers [38]. Hence, the nonlinear dynamical mechanisms governing these phenomena are currently the focus of intense theoretical, numerical and experimental study. It is noteworthy, that contrary to the well-established Fermi–Pasta–Ulam problem where the dynamics is smooth [3], problems in ordered granular media are much more complex due to potential non-smoothness effects that give rise to responses that are quite unique in the class of dynamical systems [37].

The nonlinear mechanisms for achieving efficient passive shock mitigation in coupled granular chains were first studied by Starosvetsky et al. [38], who analyzed the intrinsic dynamics of two weakly coupled, strongly nonlinear granular chains mounted on linear elastic foundations with no precompression. Three different mechanisms for complete and recurrent energy exchanges between the chains were identified, namely standing and propagating breathers and traveling waves. Furthermore, it was shown both theoretically and experimentally that pulses that initially are localized to one of the chains, gradually 'spread' to all connected chains, so that ultimately pulse equi-partition occurs [39,40]. These findings open a new avenue for optimally designing granular acoustic metamaterials for energy focusing and defocusing, as well as for directed energy transfer and redirection. Hasan et al. [17] extended this concept and formulated analytically the required fully passive control law so that energy initially induced to one of the granular chains can be fully redirected in a neighboring connected chain into a one-way, irreversible fashion. Interestingly enough, the mechanism governing this design is the macroscopic analogue in space of the Landau-Zener (or tunneling) quantum mechanical effect in time, whereby, an initial state of traveling breathers in the two coupled chains (the 'donor' and the 'receiver') is gradually transformed through the variation of the spatial elastic foundation of the granular chain to a final state with a single breather propagating in only one of the chains (the receiver).

When constructing practical granular networks (for a detailed introduction to different types of engineered materials we refer to [13,35]) composed of a number of connected granular chains, there are different ways to achieve coupling between chains, e.g., by means of interstitial intruders [37,40] or by embedding the granular media in elastic or viscoelastic material matrices. Probably, the latter is the most practical and effective way to achieve such granular networks [18]. The matrix material can be chosen from a wide variety of available materials, e.g., poly-di-methylsiloxane (PDMS), silicone, urethane, geopolymer, silicone rubber, sodium- or potassium-based geopolymer, and so on. The prime advantage of using such materials is that one has the flexibility to control the coupling stiffness between the granular chains of the network by appropriate selection of the elastic and dissipative material properties of the matrix. Moreover, even for a uniform matrix material, one can also design the coupling between the chains in the network by changing the distance between chains, i.e., the amount of matrix material between them [18]. Despite the flexibility of attaining different material stiffness, embedded granular chains are convenient to construct, and practical issues, such as aligning the granules and ensuring contact between them can be systematically addressed.

An acoustic metamaterial based on coupled granular networks is a relatively new concept, and only recently has it attracted research focus. Impulsively excited such acoustic metamaterials were studied both theoretically [17,38,39] and experimentally [18], with the aim of passively redirecting propagating pulses from a directly excited chain to a single chain or a set of absorbing chains, and of identifying the nonlinear mechanisms governing these energy exchanges. However, there are no research results on granular networks under forced harmonic excitations, despite the fact that this represents an important problem of considerable practical importance in vibration isolation and other applications. The need for research in this area is further highlighted by the fact that, as shown in previous works [23,26], ordered granular chains support nonlinear acoustic bands, i.e., pass and stop-bands, in similarity to linear periodic systems. In addition, prior theoretical studies [17,21,22,38] have predicted the existence of standing and traveling breathers in such strongly (essentially) nonlinear systems, but no experimental evidence of the existence of such responses has been reported to date.

Hence, the objective of this work is to experimentally study and verify the existence of acoustic pass and stop-bands in harmonically excited single and coupled embedded granular chains, and to prove the existence of traveling breathers in these systems. We report a very rich structure of acoustic phenomena in these highly discontinuous and strongly nonlinear granular metamaterials, and prove conclusively that traveling breathers are realized robustly in granular chains embedded in three widely different types of matrices, over wide frequency and energy ranges. In addition to experimentally confirming prior theoretical predictions regarding the existence of breathers in these media, we provide a new avenue for exploring the highly complex dynamics and acoustics of granular metamaterials for a variety of practical applications.

2 Experimental fixtures, procedures and results

A set of experimental samples was constructed for the tests. In all cases granular chains consisted of 11 spherical granules (beads) composed of type 302 stainless steel (McMaster Carr®, 9291K31) of common diameter 9.5 mm embedded in a material matrix in one of two different configurations; namely, single-chain configurations (cf. Fig. 1a) and coupled-chain configurations (cf. Fig. 1b). Three different matrices were considered in the experiments, PDMS, polyurethane and geopolymer [12,24], with detailed descriptions provided below. The coupled-chain configurations each comprised of two granular chains, fabricated with their centerlines spaced at a fixed distance. By testing coupled chains with different centerline distances we were able to study energy transfer and the acoustic properties of the coupled chains as functions of their interspatial distance (or "lateral gap"). In particular, samples of coupled chains with three different interspatial distances were fabricated, with lateral gaps of 0.5, 1.5 and 2.5 mm. In order to ascertain that contact between all neighboring granules of the embedded chains was achieved in the fabrication stage, we measure the electrical resistance of each of the embedded chains with a digital multi-meter to verify continuity (contact) of the conductive granules. By doing so, we ensured that the nonlinear Hertzian law of granule-to-granule interaction was realized in each sample. This requirement is important, since any gaps between granules of the same chain would lead to significant perturbations of the measured granular dynamics.

As mentioned above polydimethylsiloxane (PDMS), polyurethane and geopolymer were used as matrices for the granular chains. The PDMS (Sylgard 184, Dow Corning®) was a silicon elastomer synthesized by mixing a polymer base and a binding agent in 10:1 ratio. At room temperature, the PDMS cured within 48 h and its resulting microstructure consisted of homogenously bonded polymer chains. The polyurethane (74-55, Polytek®) was manufactured similarly by mixing two components in a 4:1 ratio. The polyurethane cured in 24 h at room temperature. The polyurethane 74-55 was a dimensionally stable, firm rubber. The geopolymer was an inorganic polymeric material composed of alkali metal oxides, silica and alumina. In the present study, the short carbon fiber reinforced potassium geopolymer was used to form the matrix. In contrast to traditional ceramic processing involving powder synthesis, calcination and sintering, the synthesis of geopolymer is a simple process of mixing a liquid waterglass solution and metakaolin, similar to the PDMS and polyurethane [2].

The mechanical properties of these materials should be investigated to understand the matrix effect in the dynamics of embedded granular chains. The typical elastic moduli of PDMS and polyurethane are 1.2 and 25 MPa, respectively. In addition, the elastic modulus of the short carbon-fiber reinforced geopolymer composite was measured by impact excitation to be 14 GPa, which was much lower than that of alumina (350 GPa). The hardness of PDMS, polyurethane and geopolymer were 43 and 55 as measured by a durometer, shore A and 450 MPa according to the Vickers hardness test. The low viscosity of the liquid phase of the embedding materials allowed us to embed the granular chains in the matrices accurately. For a detailed exposition of the fabrication process we refer to [18].

The experimental fixture is shown in Fig. 2. Each experimental sample was placed on top of a Teflon base (sheet), with additional Teflon blocks placed on its sides. The friction provided by the contact between the Teflon sheets and the elastic matrix restricted the translational and lateral motions of the sample, and provided an effective elastic foundation to the granular chain(s) embedded in the sample. Different excitation and transduction mechanisms were adopted for each of the two chain configurations. Considering first a single-chain sample, controlled excitation to the first granule (at the left end) was applied by means of an APS® long-stroke shaker. The stinger of the shaker was guided to excite horizontally the sample, and a piezoelectric force transducer (PCB® model 208C03, with sensitivity 2,248 mV/kN) was attached at the

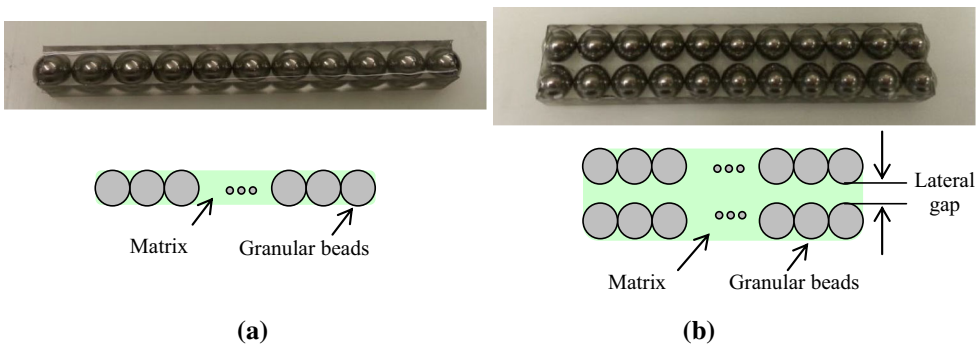

Fig. 1 Experimental samples used in the tests: (**a**) single chain embedded in PDMS matrix and corresponding schematic diagram, (**b**) coupled chains embedded in PDMS matrix with fixed lateral gap equal to 0.5 mm and corresponding schematic diagram

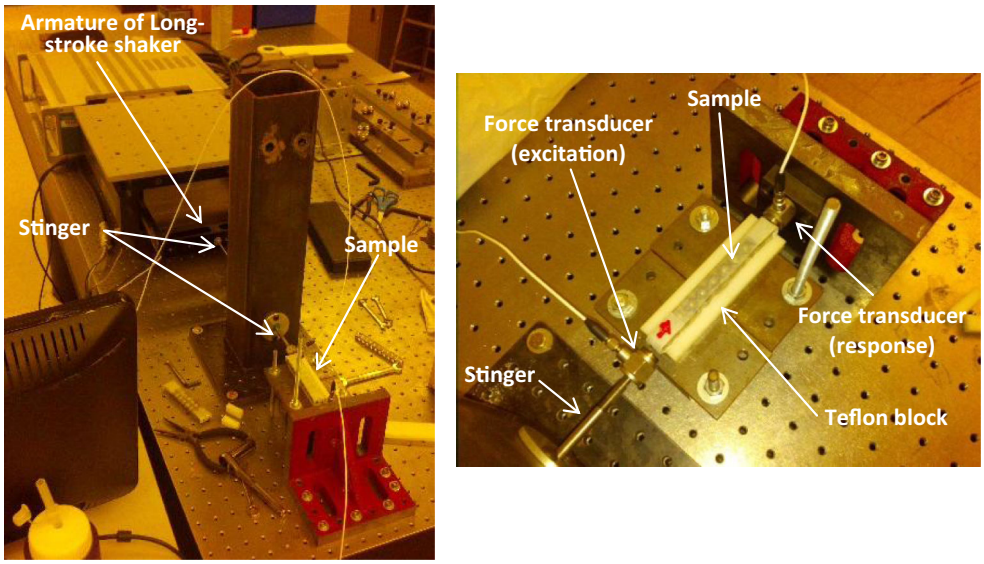

Fig. 2 Experimental fixture arranged for testing the embedded granular chains under harmonic excitation showing *side* and *top* views of the excitation and transduction mechanisms, as well as the positioning of the sample between *side* and *bottom* Teflon supports

point of contact of the stinger with the sample in order to measure the applied force. Given that the force transducer was not glued to the sample (i.e., depending on the frequency and amplitude of the excitation it could lose contact with the sample), the measured force was highly affected by the measured response, due to the strong nonlinear sample-stinger dynamic interaction during the measurement. Hence, an additional measurement was performed by recording the velocity of the armature of the shaker by means of a laser vibrometer (Polytec® model PSV-300-U), which was unaffected by the measured dynamics and enabled accurate measurement of the amplitude and frequency of the applied harmonic motion. An additional piezoelectric force transducer (PCB® model 208C02, with sensitivity 11,241 mV/kN) was used to measure the transmitted force at the right end of the sample. Hence, in tests of single embedded granular chains only two force transducers were used to measure the input and output forces for each sample.

A different excitation–transduction mechanism was used to test samples of coupled embedded granular chains. The chain directly forced by the shaker was designated as the "excited chain", whereas the other chain, placed in parallel with the excited chain, was referred to as the "absorbing chain." A harmonic input excitation was applied to the first bead at the left end of the excited chain, whereas the velocity of the last (the 11th) bead of the excited chain was measured by a second laser vibrometer (Polytec® model PSV-400). Regarding the absorbing chain, whereas its left end was contact free, its right end was placed in contact with a force transducer (PCB® model 208C02, with sensitivity 11,241 mV/kN) in order to study the force transmitted at its end. As for the case of both single and coupled embedded chains, measurement of the velocity of the armature of the shaker was performed in order to record accurately the frequency and amplitude of the excitation applied to the sample.

A final note concerns the effective static pre-compression in the embedded granular chains. As discussed in previous works [23,26], depending on the frequency and amplitude of the applied excitation, this static pre-compression can vary from nearly negligible (at low frequencies—in pass-bands), to moderate (at intermediate frequencies) and strong (at high frequencies—in stop-bands). In single granular chains this effective pre-compression was measured by recording the static load in the sample using a calibrated strain-gauge cell placed in contact with the last bead of the chain. Similarly, in samples with coupled chains we recorded the static load in the absorbing chain by placing the strain gauge cell in contact with the last bead of the absorbing chain.

In the following sections we report on three different regimes of the nonlinear dynamics of embedded granular media: Namely pass-bands (at low frequencies), traveling breathers (at intermediate frequencies) and stop-bands (at high frequencies). These regimes are robust in both single and coupled granular chains and for all three types of embedding matrices. The strongly nonlinear dynamical features of the responses in each of these regimes are studied in detail, and their implications for the mitigation properties of this class of highly discontinuous metamaterials are discussed.

2.1 Pass-bands dynamics

An initial series of tests considered single embedded chains under low frequency harmonic excitation. In previous works [23,26] it has been theoretically predicted that at low

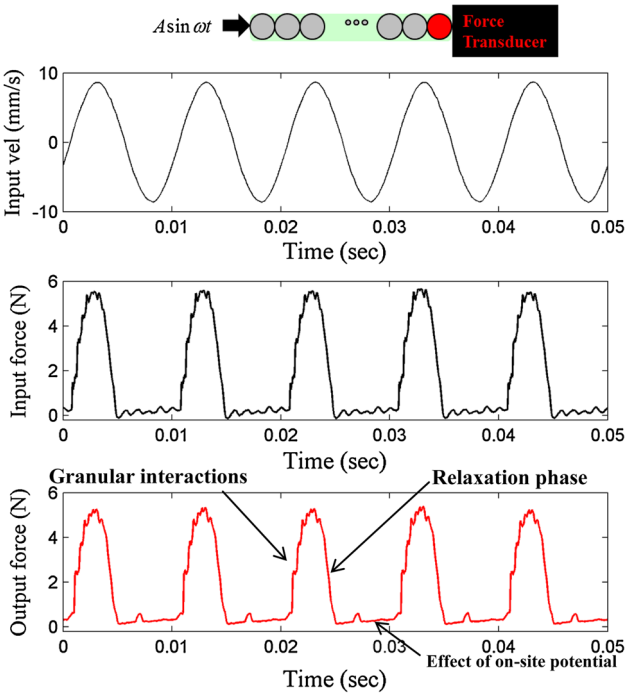

Fig. 3 Experimental velocity time series of the armature of the shaker (*top*), input force at the *left* end of the first granule (*middle*) and transmitted force at the *right* end (*bottom*) of a single granular chain embedded in PDMS matrix under relatively high amplitude excitation at 100 Hz (pass-band)

frequencies the stinger does not maintain continuous contact with the sample, so it loses contact during part of every excitation cycle and the excitation consists of a periodic series of applied pulses. As a result, a series of pulses propagates through the chain, with each pulse resembling the corresponding response for single impulse excitation. This defines a *pass-band* for the chain response, in which energy is transmitted almost unattenuated through the chain; this is verified by the series of force pulses transmitted at the right end of the sample and measured by the force transducer. We note that in the pass-band the dynamics of the chain is strongly nonlinear, and its effective pre-compression by the applied excitation is negligible.

In Fig. 3a we depict the velocity-time series of the armature of the shaker, and in Fig. 3b the corresponding measured transmitted force for a single chain embedded in PDMS matrix under harmonic excitation of relatively high amplitude at 100 Hz. The transmission of a pulse train in this medium is clearly confirmed, despite the fact that the applied harmonic excitation is continuous. Examining the waveform of a single pulse of the transmitted force, we can infer three different phases. In the first phase, corresponding to the time interval when the applied excitation is positive (i.e., the stinger of the shaker is in contact and applies a compressive force to the sample), the granules of the chain are in a state of compression against the force transducer (located at the right end of the chain). Then the granular dynamics is strongly nonlinear as Hertzian interactions between granules are realized, and this is evidenced by the non-smooth effects on the first half of the transmitted force pulse. On the contrary in the second phase where the input excitation is still positive, however the stinger relax this compressive force from the first bead of the sample, and the sample undergoes a phase of relaxation. This is evidenced by the smooth second-half of the transmitted force pulse when the granules relax and non-smooth interactions between them vanish finally. The small residual force pulses observed in-between the transmitted larger pulses in the third phase are caused by the (small) static preload realized during the first-half of the applied pulse and the presence of on-site (elastic foundation) potential in the sample because of the surrounding PDMS matrix and its friction against the supporting Teflon sheets. As a result, in the third phase the last bead does not fully relax due to the foundation effect and so regains contact with the transducer at its right end, resulting in the small force pulse. In fact, we expect that by increasing the amplitude of the excitation (keeping the frequency fixed) this residual pulse should weaken since the stronger transmitted force pulse would overcome the effects of the on-site potential of the sample; whereas when the excitation amplitude decreases the residual on-site potential effects should become more dominant as the transmitted pulse weakens, and the low-frequency resonance (ringing) of the sample as a whole should be stronger. Hence, we find that the waveforms of the transmitted low-frequency force pulses carry significant information regarding the strongly nonlinear dynamical interactions between granules and the overall interaction of the sample with its supports.

The enhanced effect of the elastic foundation on the dynamics in the pass-band is highlighted by the experimental results of Fig. 4, where the transmitted force pulses in the sample forced with smaller amplitude excitations at 100 Hz are presented. We note that in these cases the foundation effects are evidenced by small residual oscillations following the transmission of the main force pulse. For smaller excitation amplitudes, the foundation stiffness effects dominate, and the width of the pulse decreases below half the drive period. On the other hand, when the driving force amplitude increases the pulse width also increases and tends to become equal to half the period of the applied excitation. When the excitation amplitude is further increased, the forced dynamics of the embedded granular chain completely overcomes the on-site potential (foundation) effects, and the forced response behaves similar to the well-studied pulse propagation in the corresponding dry chain (i.e., the chain without the surrounding matrix). In that case the response of each granule follows the applied excitation as found in [26]. Moreover, for both low- and high-amplitude excitations, we can clearly deduce the presence of higher harmonics in the forced response. These higher harmonics are caused by the strongly nonlinear

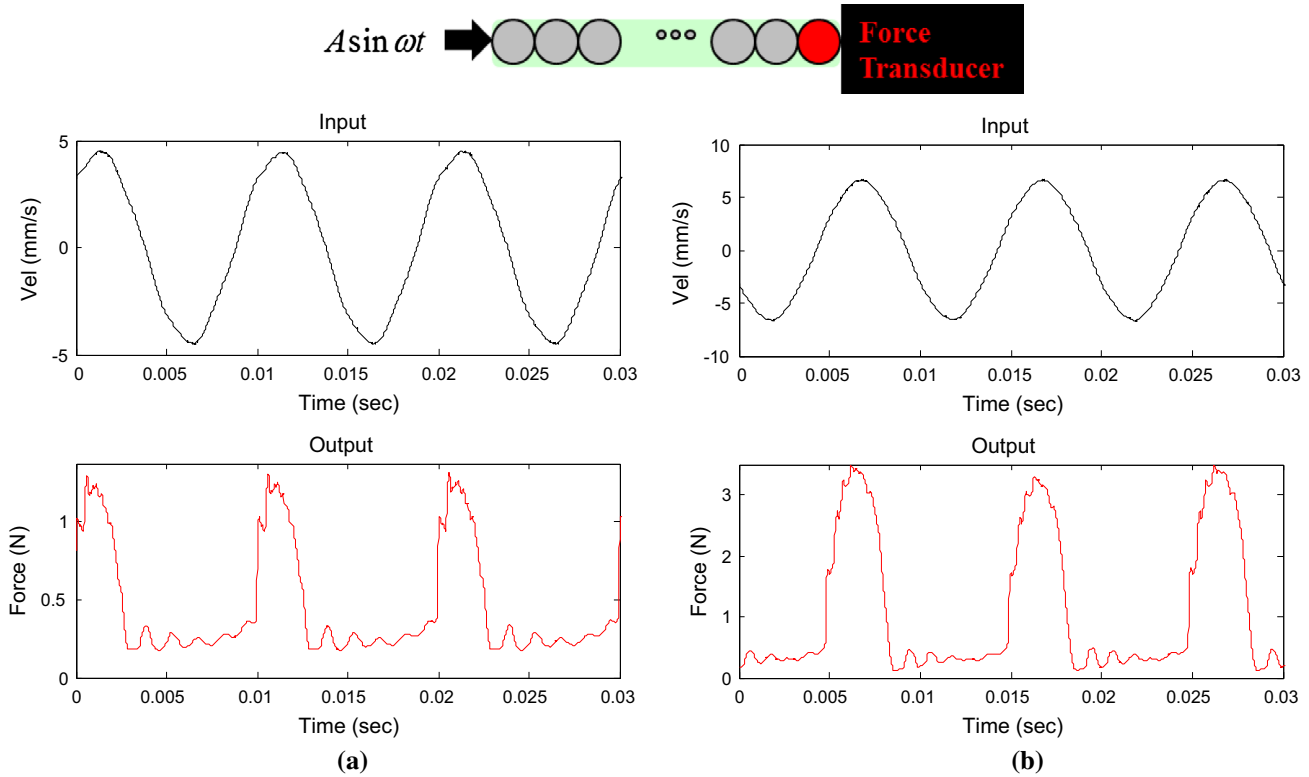

Fig. 4 Experimental velocity time series of the armature of the shaker and transmitted force at the *right* end of a single granular chain embedded in PDMS matrix for 100 Hz excitation frequency (pass-band): (**a**) Low harmonic excitation input, (**b**) medium harmonic excitation input; note the stronger effects of the on-site potential as manifested by 'ringing' of the sample after the main pulses

dynamic Hertzian interactions that occur between granules of the chain, and to separations and ensuing collisions between granules. However, the amplitudes of these higher harmonics decrease when the amplitude of excitation increases, and stronger compressive forces between granules are realized, preventing bead separations.

In a second series of experiments we studied the pass-band dynamics of coupled chains embedded in three different types of matrices, namely PDMS, polyurethane, and geopolymer, with identical lateral gaps of 0.5 mm and for identical harmonic excitations at 100 Hz; the results are depicted in Fig. 5. As reported by Hasan et al. [18] (where experimental study of similar impulsively excited embedded granular chains was performed), if two ordered granular chains are coupled through embedding common matrix, they exchange energy; moreover, the higher the coupling stiffness between chains is, i.e., the stiffer the matrix, the higher the resulting energy transfers are. This is confirmed by the experimental results of Fig. 5, where we deduce that for the chains embedded in geopolymer matrix higher energy transfer from the excited to the absorbing chain occurs, as evidenced by the higher-amplitude force transmitted by the last granule of the absorbing chain; at the same time the velocity pulse measured at the last granule of the excited chain is the lowest in amplitude compared to the other two cases. Moreover, for the chain embedded in PDMS matrix, the energy transfer between chains is the lowest.

It is interesting to note that in the pass-band of the coupled chains similar pulse-like behavior for the transmitted force to the single chain system is observed, indicating highly nonlinear dynamic response and small effective pre-compression. In addition, the effects of granular interactions are again evident in the form of non-smooth effects in the first-halves of the force and velocity pulse, followed by relaxation and on-site potential effects. As in the case of the single embedded chain, the on-site potential (or elastic foundation) effects are caused by adhesion or friction of the surrounding matrix to the supporting Teflon blocks, giving rise to an elastic restoring (foundation) effect. Moreover, although the three materials used as matrices have drastically different stiffness and dissipation properties, the measured velocity and transmitted force wave patterns are similar (albeit of varying intensity), which highlights the robustness of the granular media dynamics for varying embedding media. This robustness of the granular media dynamics is a common feature in our study and extends to the stop-bands as well as to regimes of breathers formation.

An additional series of experiments has been performed to study the pass-band dynamics of coupled granular chains embedded in PDMS matrix, but in samples with varying lat-

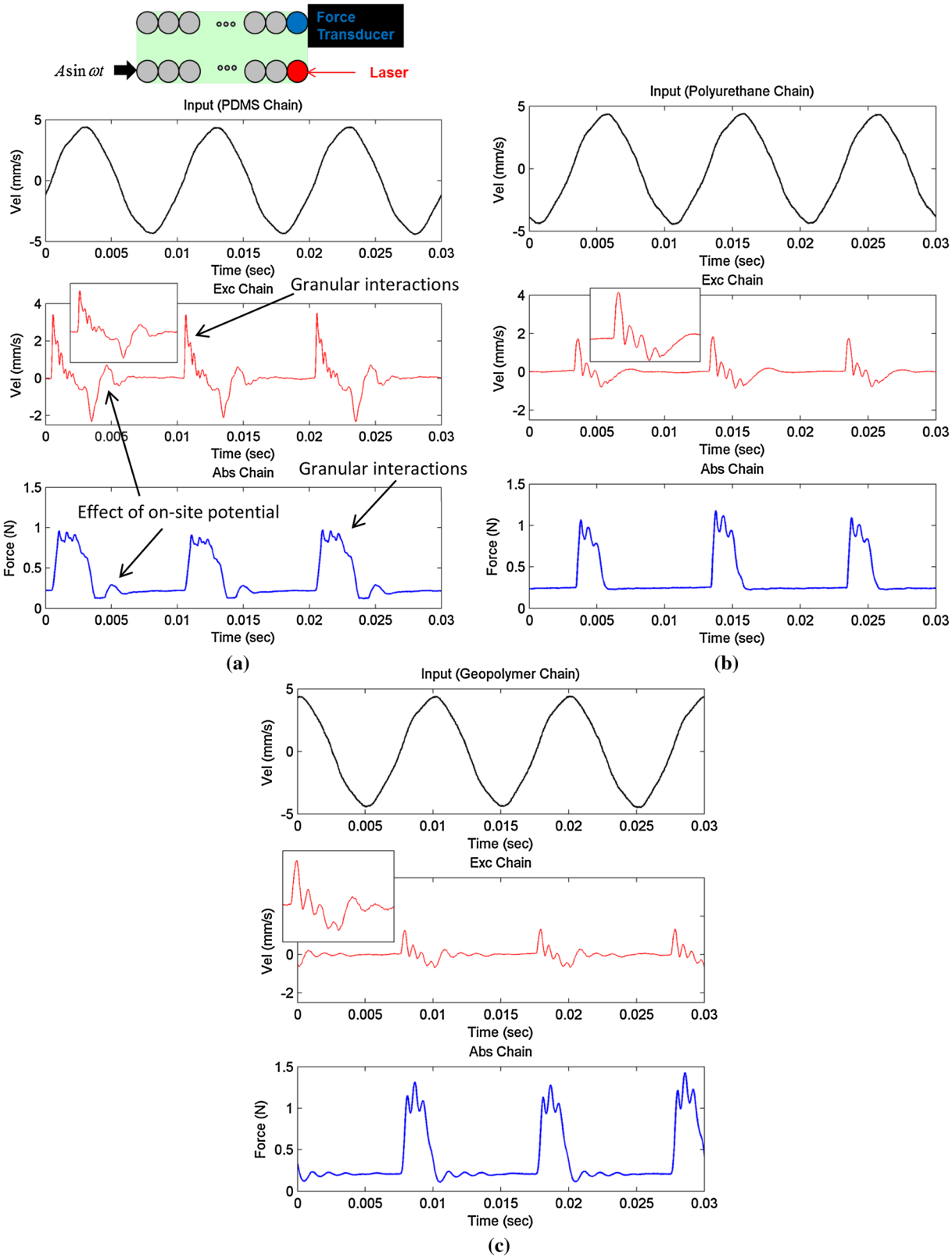

Fig. 5 Pass-band responses of three coupled chains embedded-in-matrix with 0.5 mm lateral gap under identical harmonic excitation at 100 Hz: (**a**) chain embedded in PDMS matrix, (**b**) chain embedded in polyurethane matrix, and (**c**) chain embedded in geopolymer matrix; in each case we depict the velocity time series of the armature of the shaker (*top*), the velocity of the last granule of the excited chain measured by a laser vibrometer (*middle*), and the force transmitted by the last granule of the absorbing chain (*bottom*)

eral gaps of 0.5, 1.5 and 2.5 mm. Again, for each test case harmonic excitation with fixed amplitude and a frequency of 100 Hz is applied to the excited chain, and the velocity of the last granule of the excited chain, as well as the force transmitted by the last granule of the absorbing chain are recorded. The results are presented in Fig. 6, and interesting conclusions regarding the effect of the lateral gap on the dynamics can be inferred. We deduce that (similarly to the results presented in [18]), the smaller is the lateral gap, the higher is the resulting energy transfer between the excited and absorbing granular chains. This should not be surprising given that smaller amount of matrix between the chains facilitates the energy exchange between them (predominantly through coupling shear forces [18]), whereas the coupling forces are expected to diminish as more matrix material exists between the chains (when the lateral gap increases). We note that despite the varying lateral gap, the non-smooth effects caused by granular interactions can be clearly discerned in all cases in the first-halves of the velocity and force pulses, which indicates the robustness and persistence of granular dynamic phenomena even in coupled chains with relatively large lateral gaps. We note, however, that for the sample with the largest lateral gap (cf. Fig. 6c) the effects of granular interactions diminish in the transmitted force pulses in the absorbing chain, whereas they are enhanced in the velocity pulses in the excited chain. We conjecture that by increasing the matrix material between the granular chains, the non-smooth effects in the response of the absorbing chain are decreased due to increased dissipation and scattering of the transmitted elastic waves from the excited chain to the absorbing one, as they are transmitted through the matrix. Finally, we note the weak effective precompression in the granular chains caused by the applied harmonic input, as evidenced by the small non-zero offsets of the transmitted force pulses in the absorbing chain.

2.2 Propagating breathers

In this section we report on the existence of a strongly nonlinear class of modulated response of the harmonically forced single and coupled embedded granular chains, namely propagating breathers. These are time-periodic oscillatory responses with highly localized envelope. Until now these responses have only been theoretically predicted in ordered granular media [17,21,22,38], except in [5,42] where under conditions of strong pre-compression, discrete breathers were experimentally observed in weakly nonlinear one-dimensional diatomic granular crystals. In the current work, breathers were experimentally detected at intermediate-frequency ranges (i.e., in frequencies between the lower-frequency pass-bands and higher-frequency stop-bands—discussed later), and were found to depend on the energy level of the dynamics (as expected for this class of strongly nonlinear metamaterials). Moreover, their presence was confirmed in all tested samples and for all three material matrices, that is, PDMS, polyurethane and geopolymer; this indicates that propagating breathers are robust in this class of highly discontinuous acoustic metamaterials, a result with significant practical implications as discussed later (e.g., in designs incorporating passive energy redirection [17]). Before proceeding to the discussion of our experimental results we provide a small digression on the concept of propagating discrete breathers in nonlinear mechanical chains.

In the physics literature a breather is defined as a standing or traveling nonlinear oscillatory wavepacket propagating in a nonlinear medium, with envelope possessing localized characteristics (either in amplitude or in slope). Discrete breathers are breathers realized in nonlinear lattices and originate due to discreteness and nonlinearity [1,14,15]. The study of nonlinear localized modes or discrete breathers is a comparatively new concept in the field of homogeneous or inhomogeneous granular chains. However, numerous works have considered stationary and traveling breathers in spatially periodic chains with *smooth nonlinearities*. In a previous study, Sen et al. [34] studied the dynamical behavior of nonlinear mass-spring chains, and observed the existence of metastable breathers. In related works by Hladky-Hennion et al. [19,20] similar localized modes in band gaps of diatomic chains of welded spheres were experimentally observed. To study nonlinear localized breathing modes in a homogeneous one-dimensional granular chain with no on-site potential, Theocharis et al. [41] applied static pre-compression in the model in an effort to create *modulational instability*, which is the main dynamical mechanism behind the creation of such localized modes, as studied in the FPU lattice [15]. Surprising enough such localized breathing modes do not exist in homogeneous granular chains and hence Theocharis et al. [41] concluded that "…in chains composed of beads of the same type, the intrinsic nonlinearity, which is caused by the Hertzian interaction of the beads, appears not to support localized, breathing modes…". However, by adding an impurity bead, they observed the formation of localized breathing modes near the defect, caused by the interplay between nonlinearity and disorder. Similar discrete breathers were also observed in strongly pre-compressed diatomic chains [5,42].

As mentioned previously, ordered granular media with no pre-compression represents a class of essentially nonlinear (i.e., non-linearizable) spatially periodic dynamical systems with no linearized acoustics or dynamics, so they are expected to be highly degenerate dynamical systems. However, any initial pre-compression or any effective pre-compression caused from their intrinsic nonlinear dynamics would introduce a static preload; in turn, this would eliminate the essentially nonlinear behavior and introduce a linear component in the dynamic interactions between granules. Then, one would expect that the nonlinear dynamics of these media would be able to support the formation of

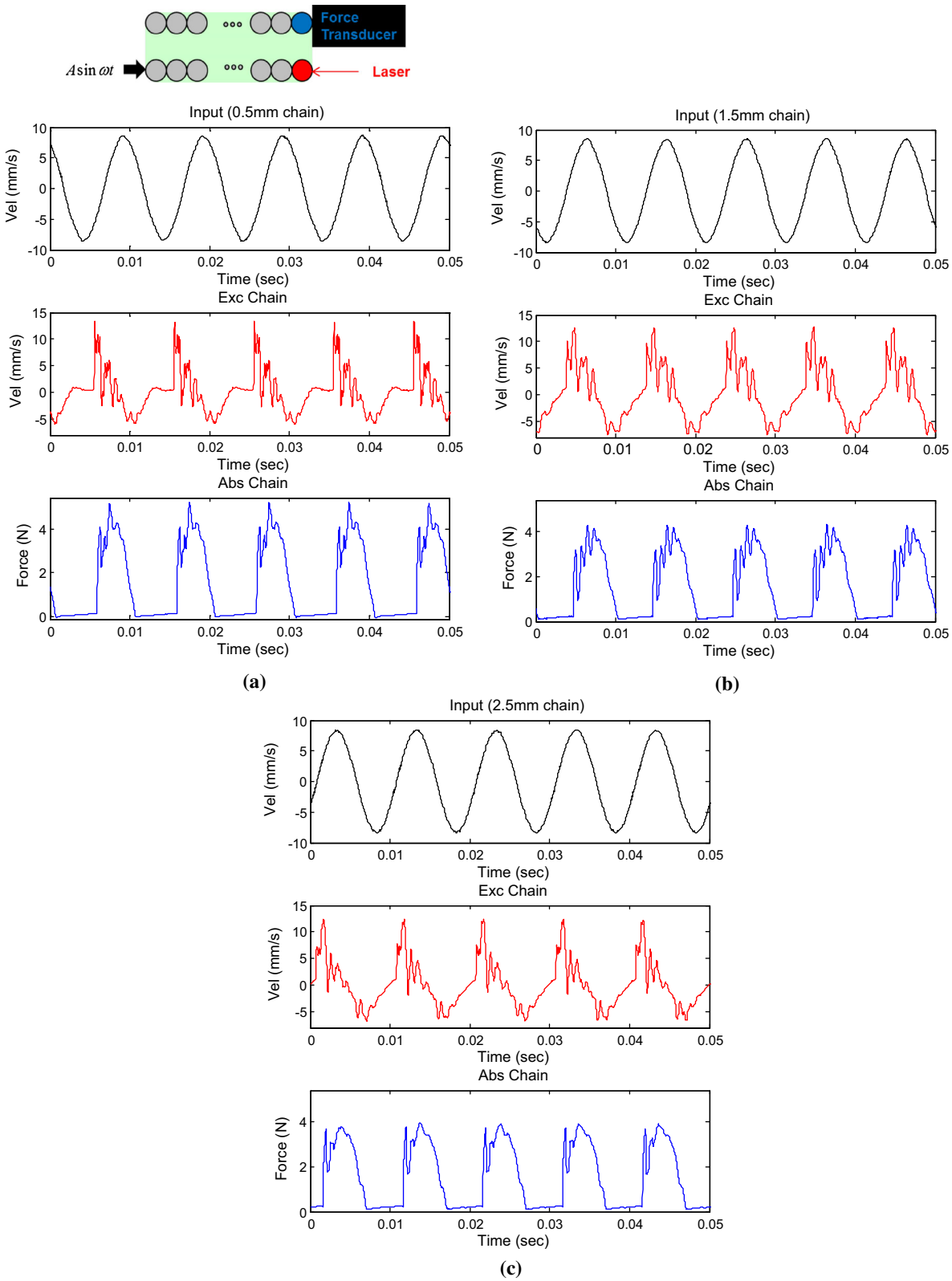

Fig. 6 Pass-band responses of three coupled chains embedded in PDMS matrix with varying lateral gap under identical harmonic excitation at 100 Hz: (**a**) 0.5 mm gap, (**b**) 1.5 mm gap, and (**c**) 2.5 mm lateral gap; in each case we depict the velocity time series of the armature of the shaker (*top*), the velocity of the last granule of the excited chain measured by a laser vibrometer (*middle*), and the force transmitted by the last granule of the absorbing chain (*bottom*)

propagating discrete breathers, in accordance with the predictions of the aforementioned studies considering chains with smooth nonlinear characteristics. Yet, as shown in [26], with increasing frequency the time-periodic response of homogeneous granular chains itself introduces effective pre-compression in these media, which increases with increasing frequency (reaching maximum pre-compression and nearly linearized dynamics in the high-frequency stop-bands). As a result, at intermediate frequency ranges (representing transitions between pass and stop-bands) it is expected that the intrinsic pre-compression developing by the intrinsic dynamics of the embedded granular chains would enable the realization of propagating breathers. This is exactly what we observed experimentally, by detecting highly nonlinear propagating discrete breathers in the form of well-defined traveling wave packets possessing highly localized envelopes.

Another comment should be made regarding the effect of the on-site potential and the discreteness of the tested material systems on the formation of propagating breathers. It is well known that discrete breathers are caused by nonlinearity and discreteness. In a series of works [17,21,22,38] it has been proven analytically and numerically that if an on-site potential exists in an uncompressed granular chain, then localized modes or breathers can be excited in that medium. Research in this field has been carried out only for impulsive excitation, and it was found that to excite breathers in such a granular chain, the strength of the on-site potential should be of the same order of magnitude or higher than the intensity of the Hertzian interaction between granules; that is, the characteristic time scale of the oscillations caused by the on-site potential (or elastic foundation) should be comparable to the characteristic time scale of the (local) dynamics of the inter-granule interactions. It follows that the existence of an on-site potential is one of the pre-requisites (together with the presence of stiffness nonlinearity) for the formation of breathers in the strongly nonlinear ordered granular media under consideration. In the experimentally tested embedded granular chains studied in this work the elastic foundation effect was realized by the matrix and the supporting Teflon sheets, so the aforementioned pre-requisite was met.

To detect propagating discrete breathers in the samples composed of single and coupled embedded chains, we first performed broad frequency sweeps of the applied harmonic excitation while also varying its amplitude. The measured waveform of the transmitted force at the end of the excited chain (for the case of a single chain) or the absorbing chain (for the case of the coupled chain, in which case the velocity waveform of the last granule of the excited chain was also measured) was carefully monitored until the sought modulated oscillatory wavetrains signaling the formation of propagating breathers could be detected. As mentioned previously propagating discrete breathers were detected in all tested samples (that is for single as well as coupled granular chains and for all three matrix materials), provided that the excitation frequency was carefully selected in the required intermediate frequency range, and the excitation amplitude was tuned accordingly.

Considering first the case of a single granular chain embedded in PDMS matrix discussed in Sect. 2.1, we have characterized a pass-band for this system as the low-frequency range where pulse-like force transmission is realized. By increasing the frequency of excitation this regime gradually vanishes, and at a range close to 400 Hz, a propagating breather in the transmitted force is realized in the form of a modulated oscillatory wavetrain with slowly varying (modulated) envelope. The time series of the measured transmitted force, as well as the corresponding spectral power density are presented in Fig. 7. This modulated response is the product of constructive interference of right-propagating and reflected left-going oscillatory waves emanating from the boundaries of the sample, and indicates the presence of modulational instability, which is the source of breathers formation in the granular chain.

It is important to note that this instability did not occur due to any electrical noise present in the electrical networks used in the experimental setup (as reported in [28]) nor to any modulation in the applied excitation (such as, frequency [28] or amplitude modulation [16]); this is clearly shown by the harmonic applied input excitation depicted in Fig. 7. Rather, the observed modulational instability is caused by the balance of competing dynamical effects, such as, the elastic foundation of the sample, the strongly nonlinear Hertzian interactions between granules and the effective pre-compression and discreteness of the granular chain. This last effect explains the formation of propagating discrete breathers at intermediate (and not lower or higher) frequency ranges: The necessary dynamical balance dictates moderate (that is, not nearly negligible as in pass-bands, nor too high as in stop-bands) effective pre-compression, leading to the dynamical formation of long-lived and spatially localized breather structures [5,42]. The manifestation of modulational instability in the experimental breather measurements is clearly visible when considering the power spectral density plot of the transmitted force in Fig. 7, from which we can deduce that in addition to the dominant harmonic component at 400 Hz, there exist side bands due to the slow modulation of the envelope of the oscillation; the existence of these side bands is a clear indicator of modulation instability in the formed wave packets. For this case, the instability growth rate is high enough to create modulational instability in the transmitted force [10,11].

From a physical point of view, the state of the breather can be regarded as an intermediate dynamical stage between the highly nonlinear and highly localized propagating pulse-like (and not oscillatory) dynamics realized in pass-bands, and the weakly nonlinear but highly attenuated oscillatory (and non-propagating) dynamics realized in stop-bands.

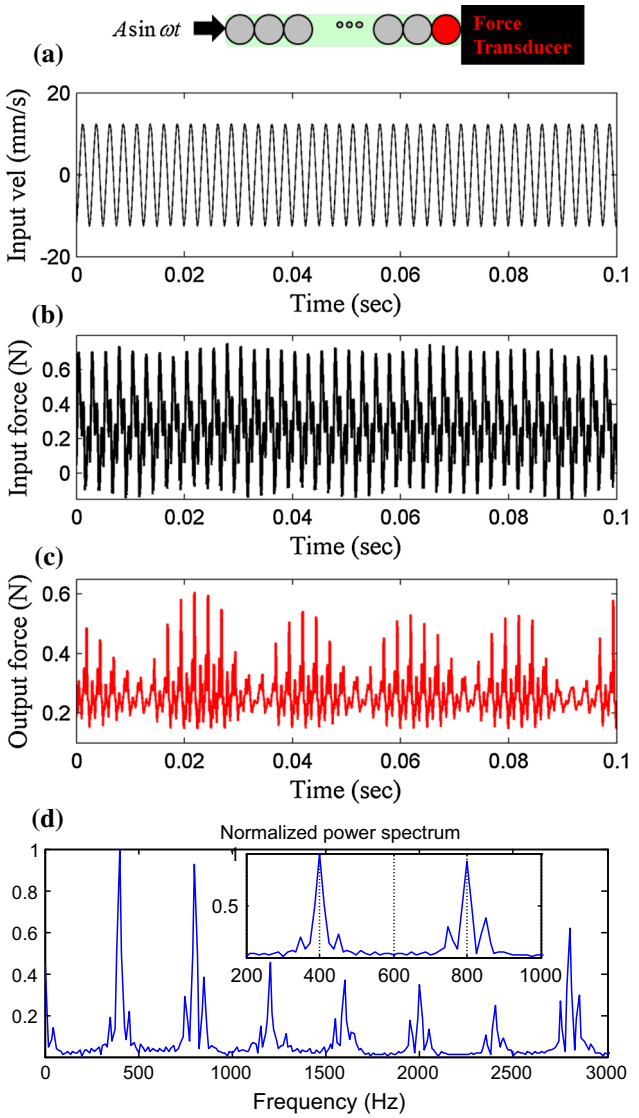

Fig. 7 Propagating breathers in the single chain embedded in PDMS matrix for harmonic excitation at 400 Hz: (**a**) Velocity time series of the armature of the shaker, (**b**) input force at the *left* end of the first granule, (**c**) force transmitted by the last granule of the chain, and (**d**) power spectral density of the force transmitted

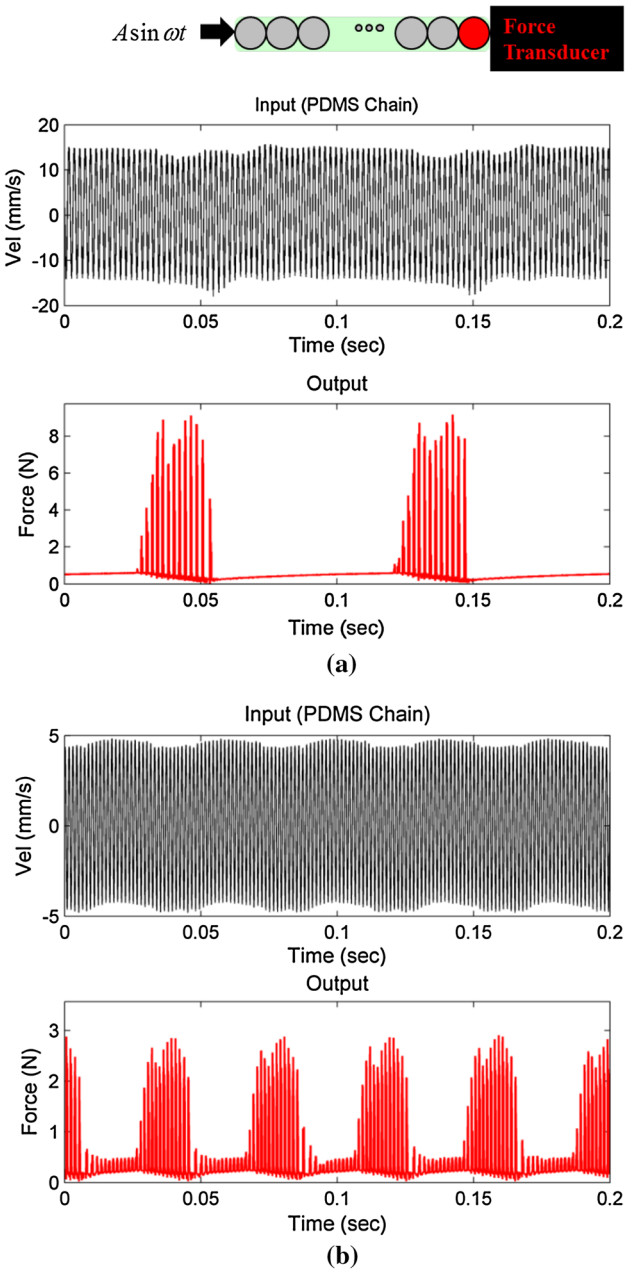

Fig. 8 Propagating breathers in the single chain embedded in PDMS matrix for harmonic excitation at (**a**) 500 Hz, and (**b**) 700 Hz; velocity time series of the armature of the shaker (*top*), and force transmitted by the last granule of the chain (*bottom*)

Hence, as transitions between these two regimes, propagating breathers are an intermediate dynamical state combining features from both of pass and stop-band dynamical states: They are strongly nonlinear, propagating and oscillatory states possessing localized envelopes. We emphasize that nonlinearity, discreteness and on-site potential are prerequisites for the realization of this type of responses.

In the performed experiments propagating breathers were quite robust for the single chain embedded in PDMS matrix, since they persisted in tests over a relatively broad frequency range.

In fact by tuning the frequency and amplitude of the applied excitation we were able to further enhance the localization of the transmitted oscillatory wavepackets by introducing 'silent regions' between them. Increasing the excitation frequency from 400 to 500 Hz, the modulational instability intensifies leading to a corresponding increase in the envelope modulation of the response of the granular chain (cf. Fig. 8a). Moreover, due to enhanced modulational instability, there occurs self-steepening of the propagating oscillatory wavetrains, resulting in the formation of discrete breathers with clear silent zones between the localized propagating

wavepackets; this is clearly evident from the experimental measurements depicted in Fig. 8a. Further increase of the excitation frequency to 700 Hz does not eliminate the propagating breathers, but 'pollutes' the silent regions between the localized propagating oscillatory wavepackets, as small-amplitude oscillations appear in these regions (cf. Fig. 8b). Nevertheless, the propagating breather persists even at that higher frequency, a finding which demonstrates the robustness of this strongly nonlinear dynamical phenomenon. We note, however, that in order to realize these results the corresponding amplitudes of the applied excitations needed to be adjusted accordingly. This can be deduced by comparing the amplitudes of the armature of the shaker velocity responses in the three cases depicted in Figs. 7, 8a, b. The intense shaker-sample interactions during this strongly nonlinear regime of the dynamics are evidenced by the weak modulations that appear in the measured velocity time series. These interactions increase the effective pre-compression of the embedded granular chain in this dynamical regime.

Increasing the excitation frequency to values higher than 700 Hz the modulational instability is gradually eliminated, and we no longer observe the propagation of breathers in the form of localized modulated propagating wave packets. Then the dynamics enters a different regime, namely a stop-band, where the embedded granular chain undergoes standing wave oscillations that are spatially localized in the vicinity of the point of the excitation and decay exponentially away from it. This results in further increase of the effective pre-compression of the embedded granular chain by the shaker and the dynamics becomes weakly nonlinear [26]. The transition from the propagating breather to this type of strongly localized response is realized by increasing the frequency and decreasing the amplitude of the applied excitation. The corresponding dynamical regime is examined in detail in Sect. 2.3. Next, we consider embedded coupled chains and prove the existence of propagating breathers in these more complex granular media as well. In particular, we prove persistence of propagating discrete breathers in samples with different matrices, and study the effect on these motions of varying the lateral gap between the chains for the same surrounding matrix.

Hence, a separate series of tests was conducted with samples of coupled granular chains under the forcing protocol described in the introduction of Sect. 2. In the first series of experimental runs we considered harmonic excitations of fixed amplitude at a fixed frequency of 500 Hz. We tested three samples of coupled chains composed of PDMS, polyurethane and geopolymer matrices and with a fixed lateral gap of 0.5 mm between the granular chains. We were able to robustly excite propagating breathers in all tests, as the results depicted in Fig. 9 clearly indicate. We note that the transmitted force measurements are highly asymmetric, due to the fact that only compressive force can be measured by the force transducer located at the end of the absorbing chain (since the transducer cannot perform a force measurement once the granular chain separates from it). Nevertheless, the presence of propagating breathers in the absorbing chain can be clearly deduced by these experimental measurements. We note that the velocity time series of the last beads of the excited chains provide the complete structure of the propagating breathers, since they are obtained by non-contacting laser vibrometry.

Interestingly enough in all measured breathers clear silent regions were recorded between propagating localized wavetrains. An indication of the strongly nonlinear dynamics of this regime is the fact that the silent regions in the transmitted forces and velocity profiles are realized even though the harmonic excitation of the excited chain is continuously applied. In addition, the multi-frequency harmonic content in the propagating wavetrains is evident in the measured time series.

From these measurements, the effects of the different matrices on the propagating breathers are deduced. First, we observe that the silent regions are smallest for breathers in the PDMS embedded chain and largest for breathers in the polyurethane embedded chain. Second, judging by the corresponding amplitudes of the measured modulated time series, we deduce that for the chains embedded in geopolymer matrix highest energy transfer from the excited to the absorbing chain is realized, whereas lowest energy transfer is realized for chains embedded in PDMS matrix; this conclusion is consistent with what was observed in the pass-band dynamics of these media, as reflected in the results of Fig. 5.

Finally, the type of matrix appears to affect the frequency content of the waveforms of the propagating breathers (especially the velocity time series of the last granules of the excited chains), with the highest frequency content appearing in the modulated dynamics of the coupled chain embedded in PDMS matrix and the lowest frequency content in the coupled chain embedded in geopolymer matrix (see also the breather comparisons in Fig. 11). This may be attributed to the much higher stiffness of the geopolymer, compared to PDMS and polyurethane. In conclusion, the material properties of the embedding matrix appear to affect drastically the waveforms of the propagating breathers, but not their realization, which is robust in samples with very dissimilar matrices.

The modulational instability that is responsible for the generation of discrete breathers in the coupled granular chain with 0.5 mm lateral gap and PDMS matrix can be clearly deduced from the results depicted in Fig. 10, where the existence of discrete breathers is manifested by the side bands close to the main harmonic components in the power spectral density of the velocity time series of the last bead of the excited chain. Also, from this power spectral density, we deduce the higher frequency content of the measured velocity

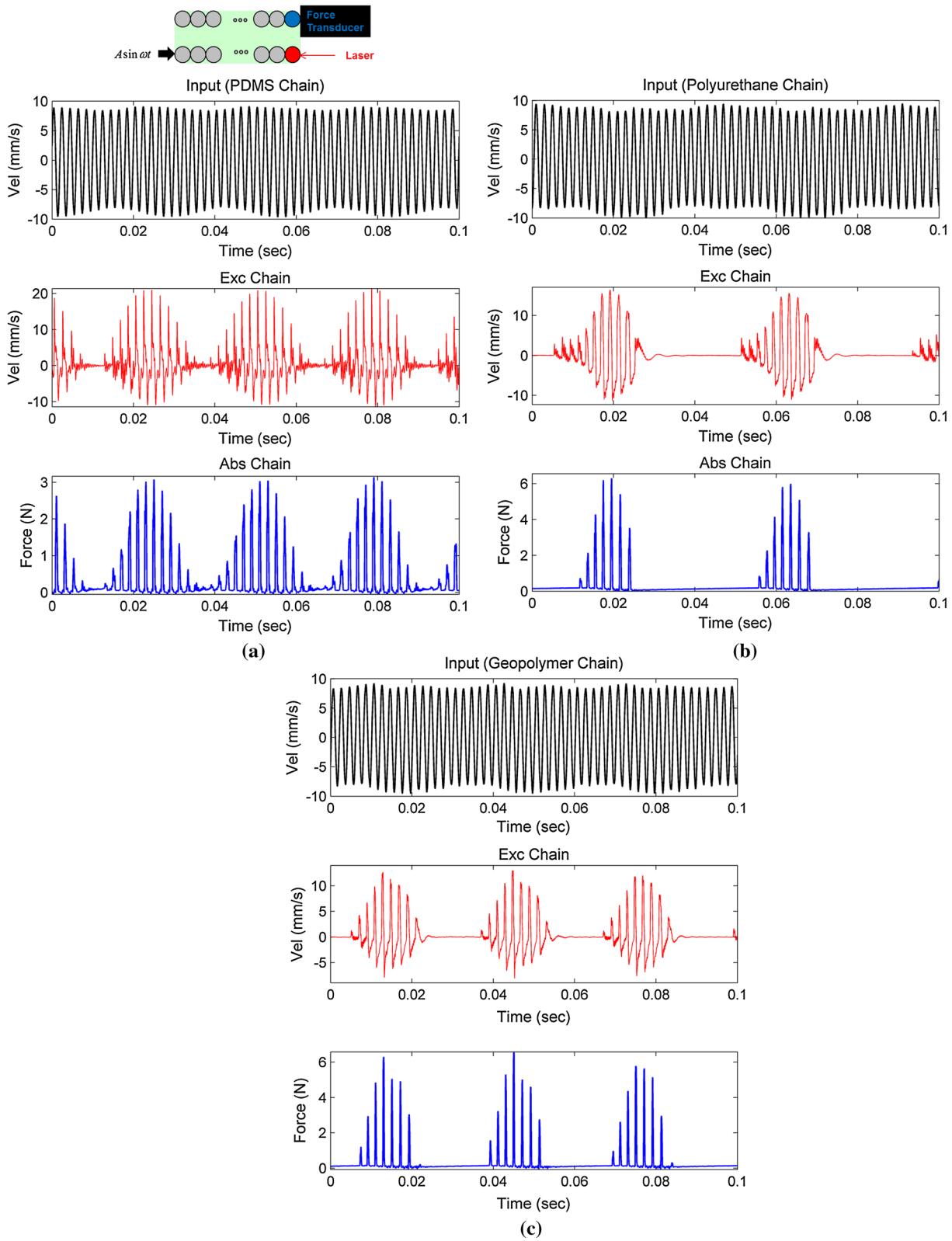

Fig. 9 Propagating discrete breathers in three coupled chains embedded in (**a**) PDMS matrix, (**b**) polyurethane matrix, and (**c**) geopolymer matrix, with fixed lateral gaps equal to 0.5 mm and common excitation amplitude and frequency 500 Hz; in each case we depict the velocity time series of the armature of the shaker (*top*), the velocity of the last granule of the excited chain measured by laser vibrometry (*middle*), and the force transmitted by the last granule of the absorbing chain (*bottom*)

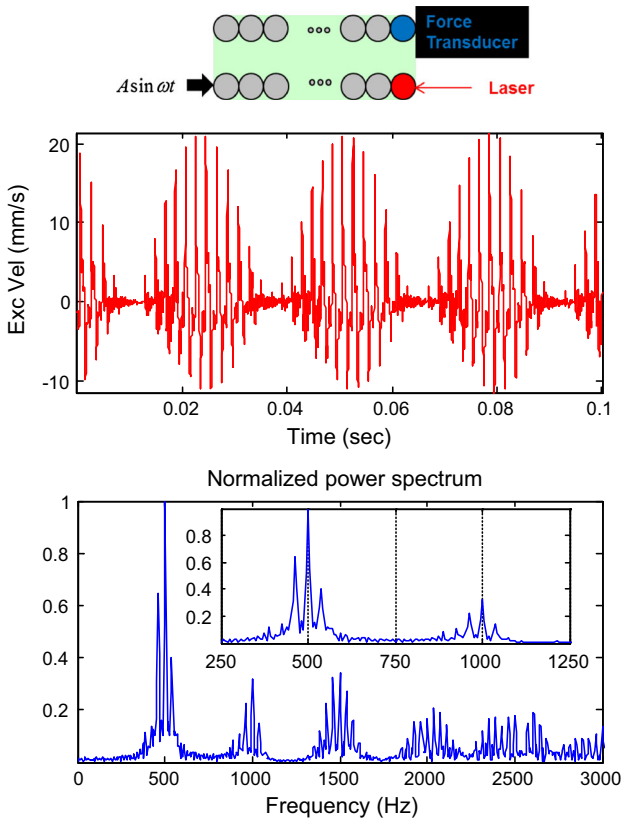

Fig. 10 Propagating breather in the coupled chain embedded in PDMS matrix with lateral gap of 0.5 mm and harmonic excitation at 500 Hz: Velocity time series of the armature of the shaker (*top*), and power spectral density of the transmitted force (*bottom*)

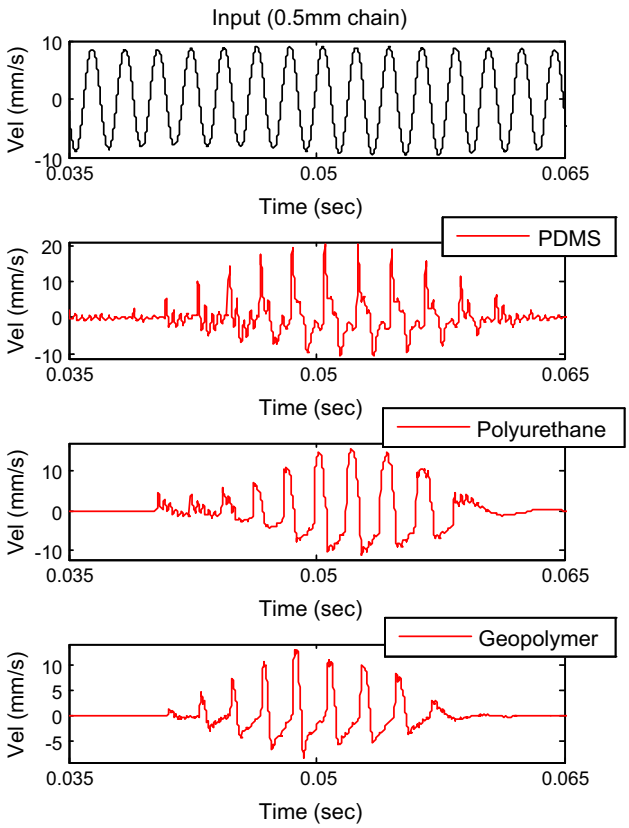

Fig. 11 Comparison of the waveforms of propagating discrete breathers in coupled chains embedded in PDMS, polyurethane, and geopolymer matrices; in all three tested samples the lateral gap was 0.5 mm, and the harmonic excitation had fixed amplitude and frequency equal to 500 Hz

time series, compared to the frequency content of the corresponding power spectral density of the propagating breather in the single chain embedded in PDMS matrix (cf. Fig. 7). This indicates that the added matrix material between the coupled chains enhances the frequency content of the propagating breather, which is in accordance to intuition given that the elastic effects of the matrix are reflected in the measured dynamics.

Another interesting feature of the detected propagating breathers is that the wavelength of the localized oscillating wavepacket appears to significantly depend on its maximum amplitude and on the material into which the granular chains are embedded. It is well known that material dissipation plays an important role on the localized shape of the discrete breathers and envelope solitons [6,15,29], since increasing dissipation decreases the amplitude of the envelope of the breather, while increasing its wavelength (i.e., the spatial extent of the localized wavepacket). Based on these predictions, and given that material damping is much higher in PDMS compared to either polyurethane or geopolymer, we can expect that the wavelength of the breather is higher in the coupled granular chains embedded in PDMS matrix than in the ones embedded in polyurethane or geopolymer. This is confirmed by the comparison of the experimental breathers in Fig. 11, where the largest wavelength is observed in the PDMS sample and the smallest in the geopolymer sample.

In a final series of experiments we studied the effect on the propagating breathers of the variation of the lateral gap in coupled chains embedded in PDMS matrix. For each of the tests we fixed the excitation frequency at 500 Hz and varied the excitation amplitude. In Fig. 12 we depict these experimental measurements for the coupled chain with 2.5 mm lateral gap, and in Fig. 13 for 1.5 mm lateral gap. These results need to be compared with the results of Figs. 9 and 11 where propagating breathers in the coupled chain with 0.5 mm lateral gap are depicted at 500 Hz excitation frequency. It is clear from Fig. 12a that no localized breathers can be excited in the chain with 2.5 mm lateral gap at low excitation amplitudes. This is clearly proved by the absence of side bands in the corresponding power spectral density of the measured velocity time series, signifying absence of modulational instability. The absence of propagating breathers can be explained when one considers that these strongly nonlinear motions are realized due to modulational instability and represent a dynamical effect of dispersion (caused by discreteness) and nonlin-

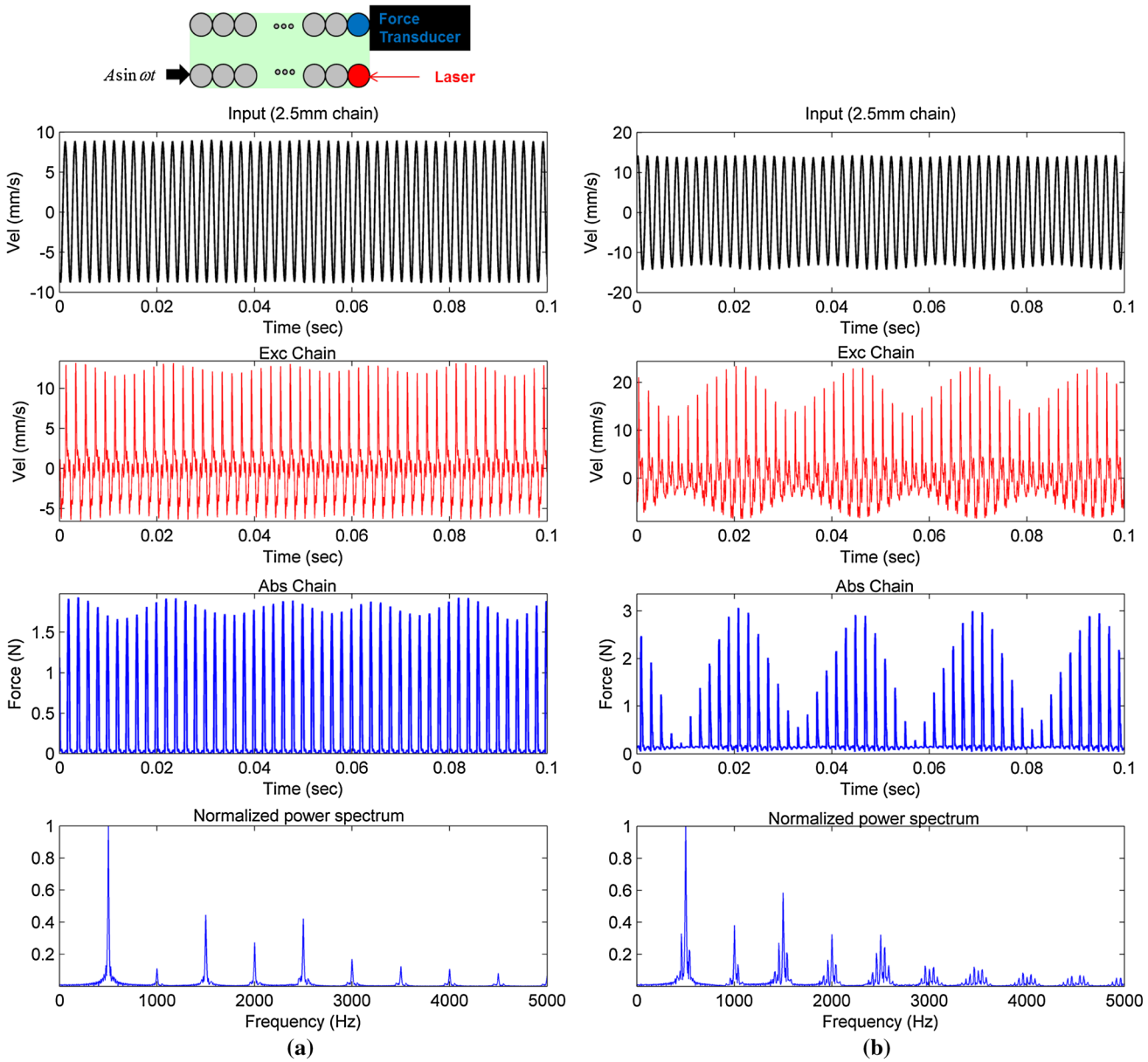

Fig. 12 Experimental response of the coupled chain embedded in PDMS matrix with 2.5 mm lateral gap and excitation frequency 500 Hz: (**a**) Absence of propagating breathers at low excitation amplitude, and (**b**) propagating breathers at high excitation amplitude; from *top* to *bottom* we depict the velocity of the armature of the shaker, the velocity of the last granule of the excited chain, the force transmitted by the last granule of the absorbing chain, and the power spectral density of the velocity of the last granule of the excited chain

earity. Hence, when the amplitude of the applied excitation (or the energy applied to the system) is not large enough, the nonlinear effects in the system with large lateral gap are less profound since energy transfers from the excited to the absorbing chain and energy transmission within each chain are weakened due to scattering in the elastic matrix between the chains, so the nonlinearity in the system is not strong enough to generate modulational instability.

It follows that to generate propagating breathers in the coupled chain with 2.5 mm lateral gap, the excitation amplitude should be increased so that the nonlinearity of the response becomes strong enough to induce modulational instability in the dynamics; this is confirmed by the experimental results of Fig. 12b where for increased excitation amplitude a propagating breather is realized, albeit with no silent regions. Indeed, for this sample with the largest lateral gap the propagating breather appears as a slowly modulated oscillation. The presence of modulational instability in the response is clearly evidenced by the rich side band structure observed in the respective power spectral density. This suggests that there is a critical excitation amplitude (or energy level) required for the initiation of modulational instability, after which the

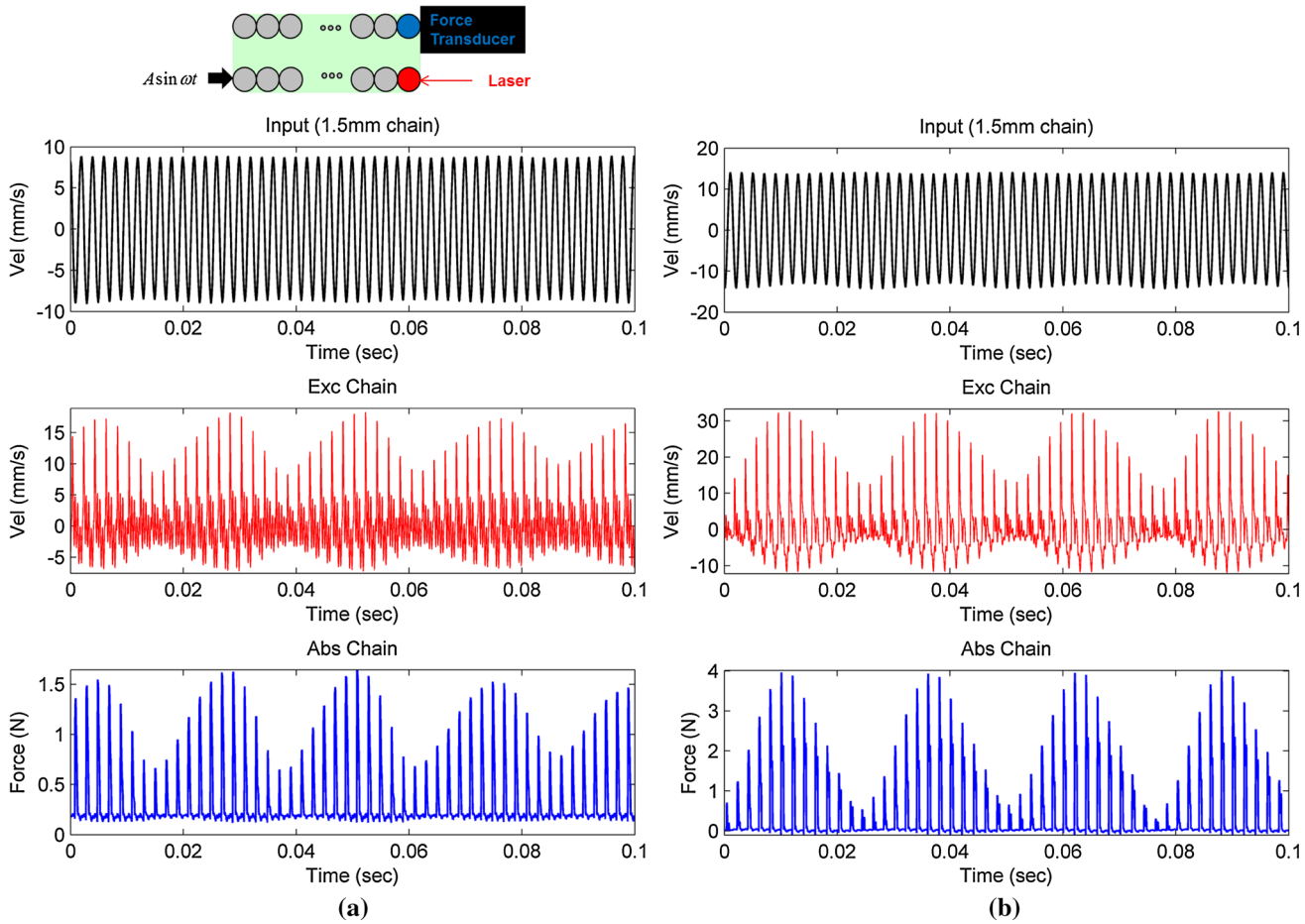

Fig. 13 Experimental measurements of propagating breathers in the coupled chain embedded in PDMS matrix with 1.5 mm lateral gap and excitation frequency 500 Hz: (**a**) low excitation amplitude, and (**b**) high excitation amplitude; from *top* to *bottom* we depict the velocity of the armature of the shaker, the velocity of the last granule of the excited chain, and the force transmitted by the last granule of the absorbing chain

spatially extended oscillations of the granular chains decay into localized discrete breathers. Our experimental finding correlates with previously reported experimental study of the formation of localized mode in one-dimensional granular media, where to excite localized mode in band gaps (i.e., in frequency ranges where no waves can be transmitted [30]) of heterogeneous granular media under harmonic excitation, the amplitude of the driving force had to be increased so that a nonlinear regime of the dynamics could be reached [4].

In Fig. 13 we depict the corresponding experimental responses for the PDMS sample with 1.5 mm lateral gap at 500 Hz excitation frequency. For this smaller gap modulational instability is excited for low as well as high excitation amplitudes. This finding demonstrates that less material matrix in-between the granular chains results in stronger nonlinear dynamical interactions between the coupled chains, and enhances the nonlinear effects during energy transmission in each chain. This can be partially attributed to the reduction of scattering effects in the dynamical interactions between the two chains due to the material matrix between them, leading to an overall enhancement of the nonlinearity in the system.

2.3 Stop-band dynamics

The dynamics of the embedded single and coupled granular chains enter a qualitatively different regime when the frequency of excitation increases further from the intermediate region of propagating breathers. In these high-frequency regimes the granular chains enter a state of strong effective compression due to the high-frequency excitation by the shaker, and the dynamics develop a predominant linear component and become weakly nonlinear. In essence, in this high-frequency regime the dynamics of the granular medium becomes almost linear, and develops the common features of linear periodic systems at high-frequencies, i.e., stop-band dynamics [26]. Then, the granular chains exhibit standing wave oscillations with exponentially decaying envelopes, localized close to the point of application of the external excitation (the shaker). Due to this localization in the stop-band

the granular medium is incapable of transmitting vibration energy in its far field, since all harmonic components are spatially attenuated due its strongly pre-compressed intrinsic dynamics. As a result, the force transmitted to its right end is greatly reduced, and the medium acts as an (almost linear) acoustic filter cutting-off all harmonics. In fact, the only surviving dynamics measured at the right ends of the granular chains correspond to the oscillatory motion of the sample as a whole, with the embedded granular chains contributing only through their inertia, with completely absent any nonlinear granular dynamic effects; then, in essence, the embedded granular chain acts as a multi-degree-of-freedom linear oscillator (depending on the modes of the matrix-chain assembly that are excited by the shaker) whose stiffness and damping properties are determined by corresponding properties of the material of the matrix, lacking any internal nonlinear granular dynamics. Key to this dynamic behavior is the state of strong effective pre-compression of the embedded granular chain inflicted by the high-frequency excitation [26], which nearly linearizes the dynamics.

This is confirmed by the results depicted in Fig. 14 for the single granular chain embedded in PDMS matrix and forced by a harmonic excitation at 5,000 Hz. We deduce that, contrary to the applied excitation, in the transmitted force there is a complete absence of high-frequency harmonic components since they are attenuated by the strongly pre-compressed granular chain. In fact, the high effective pre-compression of the chain is evidenced by the nonzero average values of both the applied and transmitted forces. The absence of high-frequency harmonic components in the transmitted force is further proved by its power spectral density and wavelet transform spectrum in Fig. 14, where the harmonic at the frequency of the applied excitation (5,000 Hz) is highly attenuated, and only low-frequency harmonics are present in the output: One harmonic component close to 50 Hz and another one close to 200 Hz. These low-frequency oscillations correspond to the low-dimensional response of the matrix-chain sample oscillating as a whole, with the granular chain contributing only by its inertia, and the matrix by its material elasticity and dissipation. We conclude that in this dynamical regime (stop-band) the embedded granular chain acts as an (almost linear) acoustic filter, preventing the transmission of energy through the granular medium by attenuating all harmonic components generated at the local site of the shaker—chain interaction. In this case the only transmitted force is due to the low-frequency vibration of the assembly as a whole, with all internal nonlinear granular interactions being dissipated by the intrinsic dynamics itself. These results highlight the high tunability of the considered acoustic metamaterial, since depending on the frequency (and amplitude) of the applied harmonic excitation its dynamics can range from strongly nonlinear and propagatory (in low-frequency pass-bands and intermediate-frequency regimes of breather formation) to almost linear, oscillatory and attenuatory (in high-frequency stop-bands). This passive tunability of the dynamics can find application in designs of a new class of highly discontinuous metamaterials usable as acoustic filters, and shock / vibration mitigators.

Similar stop-band dynamics was observed in all tested embedded coupled granular chains, for each of the three material matrices considered in our study. Representative results are depicted in Fig. 15, which clearly demonstrate the stop-band dynamics of coupled granular chains with 0.5 mm lateral gaps embedded in PDMS, polyurethane, and geopolymer matrices. This further proves the robustness of this high-frequency dynamic regime.

These results conclude our experimental study. In the next section we discuss mathematical models that were constructed to theoretically simulate the dynamics of the considered single and coupled embedded granular chains. The origin of these models can be found in [18], where energy transmission and exchange in impulsively excited coupled granular chains embedded in PDMS matrix were considered, in an effort to gain predictive design capability for the nonlinear dynamics of these systems. In the following section we focus only on the intermediate-frequency regimes of breather formation in order to show that the previous experimental results can be qualitatively recovered by models that, although simplified, are capable of capturing the important nonlinear dynamics in these regimes.

3 Theoretical modeling

In this section we provide a theoretical study that predicts the discrete breathers propagating through granular chains embedded in matrices. Although we consider only intermediate-frequency dynamics our models are capable of representing pass- and stop-band dynamics as well, but this study is omitted from further consideration. Motivated by the mathematical model first developed in [18], we approximate the experimental samples discussed previously by simplified models of coupled granular crystals consisting of either single (Fig. 16a) or coupled (Fig. 16b) one-dimensional homogeneous chains of identical elastic spherical granules initially in contact.

We assume nonlinear Hertzian interactions between interacting granules governed by the force-displacement law $f = Cd_+^{3/2}$, where d is the overlap displacement between granules, C the coefficient of the Hertzian interaction (dependent on size and material [18]), and f the resulting compressive force. The subscript (+) indicates that this expression has meaning only if $d \geq 0$, and is equal to zero otherwise; in essence, the previous relation models both the nonlinear Hertzian interaction between granules in contact and com-

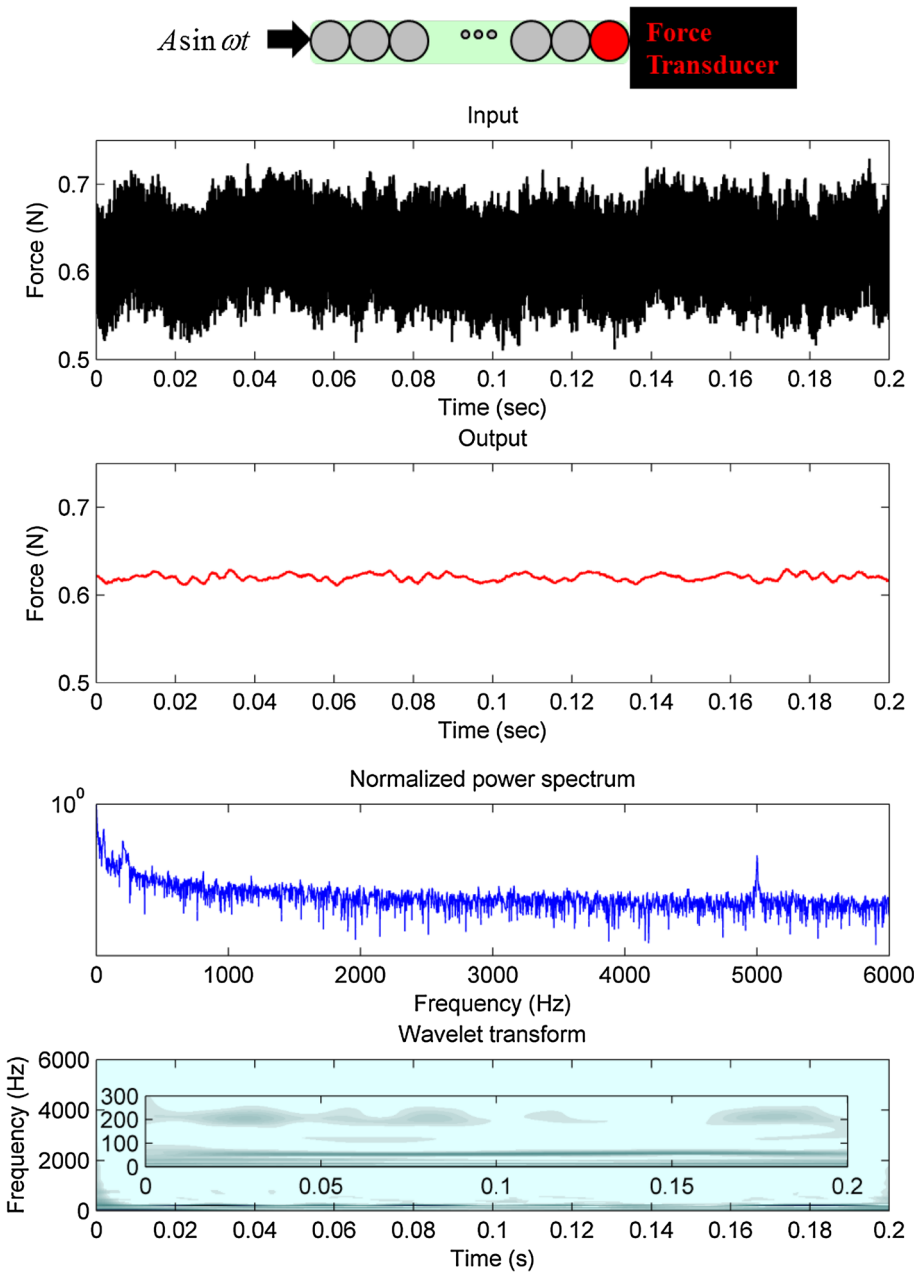

Fig. 14 Experimental response of the single chain embedded in PDMS matrix for excitation frequency of 5,000 Hz; from *top* to *bottom*: Force applied by the shaker to the first granule, force transmitted by the end granule at the right boundary, and power spectral density and wavelet spectrum of the transmitted force (*inset* shows a detail of the wavelet spectrum)

pression, and the granule separation in the absence of compressive forces and loss of contact. We note that variations or deviations from the 3/2 nonlinear exponent can cause shifts in the intermediate-frequency ranges at which propagating breathers are predicted by the models. Boechler et al. [4] studied band gaps in heterogeneous periodic chains (dimers), and carried out sensitivity analysis to study the possible causes of frequency up-shifts observed in their experimental data when compared to predicted values estimated from theory. They found that a small shift of about 1.8 % in the value of the nonlinear exponent of the Hertzian interaction law can cause an approximately 12 % shift in the predicted band frequency edges.

In the theoretical models of Fig. 16, we further assume that the granules of each chain are constrained to move only in the horizontal direction; all granules are made out of stainless steel granules with uniform diameter 9.5 mm and mass m, and that a prescribed base excitation $F(t)$ is applied to the first bead of the single chain, or the first bead of the excited chain of the coupled system. Moreover, in the model of coupled chains only local coupling (with stiffness constant k_2) between the corresponding beads of each chain is considered. This amounts to a distributed linear coupling shear spring, and as the lateral gap between the two chains decreases the effective (shear) coupling between the two chains increases, and, hence, energy exchanges between

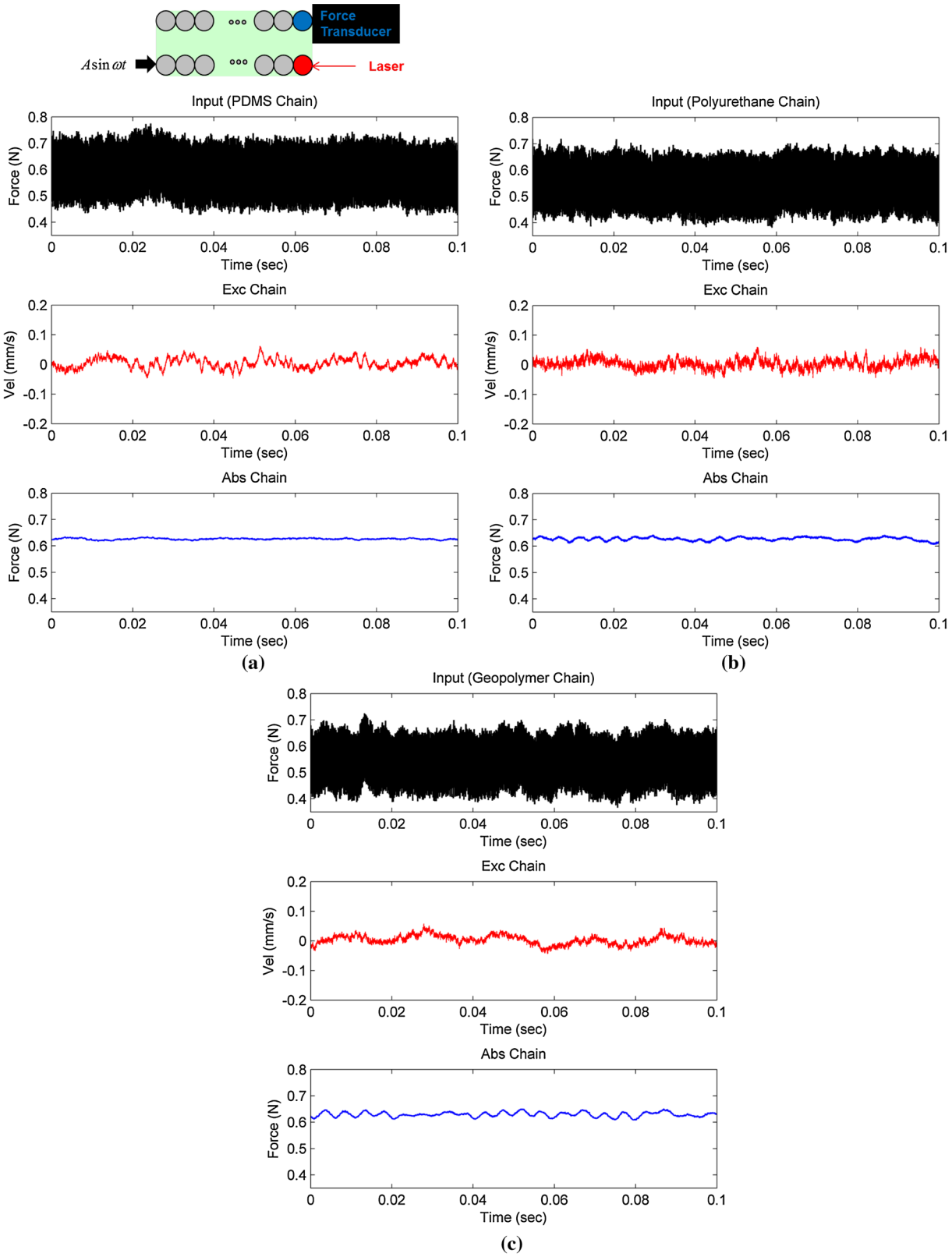

Fig. 15 Stop-band dynamics of coupled chains embedded in (**a**) PDMS matrix, (**b**) polyurethane matrix, and (**c**) geopolymer matrix, with lateral gaps of 0.5 mm and fixed excitation amplitude and frequency of 5,000 Hz; in each case we depict the force applied by the shaker to the left boundary of the excited chain (*top*), the velocity of the last granule of the excited chain measured by a laser vibrometer (*middle*), and the force transmitted by the last granule of the absorbing chain (*bottom*)

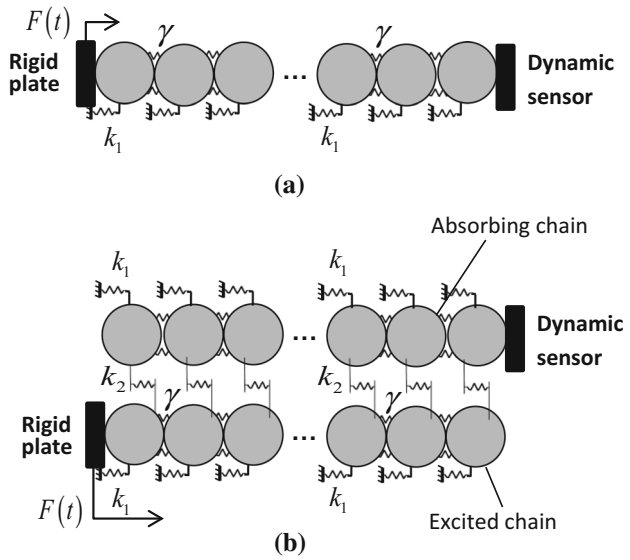

Fig. 16 Mathematical models for (**a**) a single chain, and (**b**) coupled granular chains embedded in an elastic matrix

the excited and absorbing chains become more profound. In addition, the surrounding matrix is assumed to be linearly elastic, and is modeled by introducing a linear elastic foundation (i.e., a linear on-site potential) with stiffness constant k_1 in each chain, and linear coupling springs with stiffness constant γ between interacting granules of each chain. Finally, similarly to [18], proportional viscous dissipation is imposed in order to model material damping in the surrounding matrix and dissipative effects during granular interactions in the respective experimental systems. The interaction of each granule with the surrounding matrix is modeled by the viscous damping coefficient λ_{k_1}, the dissipation during Hertzian interactions between neighboring granules by the damping coefficient λ_1, and energy losses due to coupling matrix effects between neighboring chains by the damping coefficient λ_{k_2}. Under these assumptions the governing equations of motion for the model of embedded coupled chains depicted in Fig. 16b are expressed as (similar equations hold for the model of Fig. 16a):

$$
\begin{aligned}
&m\ddot{x}_1 + k_1 x_1 + \lambda_{k_1}\dot{x}_1 + k_2\left(x_1 - y_1\right) + \lambda_{k_2}\left(\dot{x}_1 - \dot{y}_1\right)\\
&= C\left[\left(A\sin\left(\omega t\right) - x_1 + \delta_0\right)_+^{3/2}\right] - C\left[\left(x_1 - x_2 + \delta_0\right)_+^{3/2}\right]\\
&\quad + \lambda_1\left(\omega A\cos\left(\omega t\right) - \dot{x}_1\right) H\left(A\sin\left(\omega t\right) - x_1 + \delta_0\right)\\
&\quad - \lambda_1\left(\dot{x}_2 - \dot{x}_1\right) H\left(x_1 - x_2 + \delta_0\right)\\
&\quad - \gamma\left[\mathrm{sgn}\left(x_1 - x_2\right)\left|x_1 - x_2\right|\right]\\
&m\ddot{y}_1 + k_1 y_1 + \lambda_{k_1}\dot{y}_1 + k_2\left(y_1 - x_1\right) + \lambda_{k_2}\left(\dot{y}_1 - \dot{x}_1\right)\\
&= -C\left[\left(y_1 - y_2 + \delta_0\right)_+^{3/2}\right] - \lambda_1\left(\dot{y}_2 - \dot{y}_1\right) H\left(y_1 - y_2 + \delta_0\right)\\
&\quad - \gamma\left[\mathrm{sgn}\left(y_n - y_{n+1}\right)\left|y_n - y_{n+1}\right|\right]
\end{aligned}
$$

$$
\begin{aligned}
&m\ddot{x}_n + k_1 x_n + \lambda_{k_1}\dot{x}_n + k_2\left(x_n - y_n\right) + \lambda_{k_2}\left(\dot{x}_n - \dot{y}_n\right)\\
&= C\left(x_{n-1} - x_n + \delta_0\right)_+^{3/2} - C\left[\left(x_n - x_{n+1} + \delta_0\right)_+^{3/2}\right]\\
&\quad + \gamma\left[\mathrm{sgn}\left(x_{n-1} - x_n\right)\left|x_{n-1} - x_n\right|\right.\\
&\quad \left. - \mathrm{sgn}\left(x_n - x_{n+1}\right)\left|x_n - x_{n+1}\right|\right]\\
&\quad + \lambda_1\left(\dot{x}_{n-1} - \dot{x}_n\right) H\left(x_{n-1} - x_n + \delta_0\right)\\
&\quad - \lambda_1\left(\dot{x}_{n+1} - \dot{x}_n\right) H\left(x_n - x_{n+1} + \delta_0\right), n = 2, \ldots, 10\\
&m\ddot{y}_n + k_1 y_n + \lambda_{k_1}\dot{y}_n + k_2\left(y_n - x_n\right) + \lambda_{k_2}\left(\dot{y}_n - \dot{x}_n\right)\\
&= C\left(y_{n-1} - y_n + \delta_0\right)_+^{3/2} - C\left[\left(y_n - y_{n+1} + \delta_0\right)_+^{3/2}\right]\\
&\quad + \gamma\left[\mathrm{sgn}\left(y_{n-1} - y_n\right)\left|y_{n-1} - y_n\right|\right.\\
&\quad \left. - \mathrm{sgn}\left(y_n - y_{n+1}\right)\left|y_n - y_{n+1}\right|\right]\\
&\quad + \lambda_1\left(\dot{y}_{n-1} - \dot{y}_n\right) H\left(y_{n-1} - y_n + \delta_0\right)\\
&\quad - \lambda_1\left(\dot{y}_{n+1} - \dot{y}_n\right) H\left(y_n - y_{n+1} + \delta_0\right), n = 2, \ldots, 10\\
&m\ddot{x}_{11} + k_1 x_{11} + \lambda_{k_1}\dot{x}_{11} + k_2\left(x_{11} - y_{11}\right) + \lambda_{k_2}\left(\dot{x}_{11} - \dot{y}_{11}\right)\\
&= C\left(x_{10} - x_{11} + \delta_0\right)_+^{3/2} + \lambda_1\left(\dot{x}_{10} - \dot{x}_{11}\right)\\
&\quad \times H\left(x_{10} - x_{11} + \delta_0\right) + \gamma\left[\mathrm{sgn}\left(x_{10} - x_{11}\right)\left|x_{10} - x_{11}\right|\right]
\end{aligned}
$$

$$
\begin{aligned}
&m\ddot{y}_{11} + k_1 y_{11} + \lambda_{k_1}\dot{y}_{11} + k_2\left(y_{11} - x_{11}\right) + \lambda_{k_2}\left(\dot{y}_{11} - \dot{x}_{11}\right)\\
&= C\left(y_{10} - y_{11} + \delta_0\right)_+^{3/2} - C\left[\left(y_{11} + \delta_0\right)_+^{3/2}\right]\\
&\quad + \lambda_1\left(\dot{y}_{10} - \dot{y}_{11}\right) H\left(y_{10} - y_{11} + \delta_0\right)\\
&\quad - \lambda_1\left(-\dot{y}_{11}\right) H\left(y_{11} + \delta_0\right)\\
&\quad + \gamma\left[\mathrm{sgn}\left(y_{10} - y_{11}\right)\left|y_{10} - y_{11}\right|\right] \qquad (1)
\end{aligned}
$$

where $x_n(t)$ and $y_n(t)$ are the displacements of the $n-th$ granules of the excited and absorbing chains, respectively, and $H(\cdot)$ is the Heaviside function. The parameter δ_0 models the applied pre-compression of the chain scaled by the common radius of the granules, and to model the excitation applied by the shaker the prescribed base periodic excitation $F(t) = A\sin(\omega t)$ is applied to the first bead of the excited chain. Moreover, for a single chain we set the coupling parameters k_2, and λ_{k_2} equal to zero.

Based on the experimental results of Sect. 2.2, propagating discrete breathers are realized at the intermediate frequency range of 400–700 Hz for both single and coupled embedded chains. Assuming PDMS matrix, the parameters of the model are taken from [18], where related experimental tests with impulsive excitation were carried out and a systematic identification of the stiffness and damping parameters was performed. What we change in the present study are the parameters of the elastic foundation k_1 and the associated viscous damping term λ_{k_1}, given that the configuration of the experimental fixture is different. Indeed, contrary to the fixture considered in [18], in the current experimental setup, the lateral motion of the experimental sample was restricted by using additional Teflon sheets on its sides, which is expected to change the stiffness and damping properties of the foundation compared to the systems tested in [18].

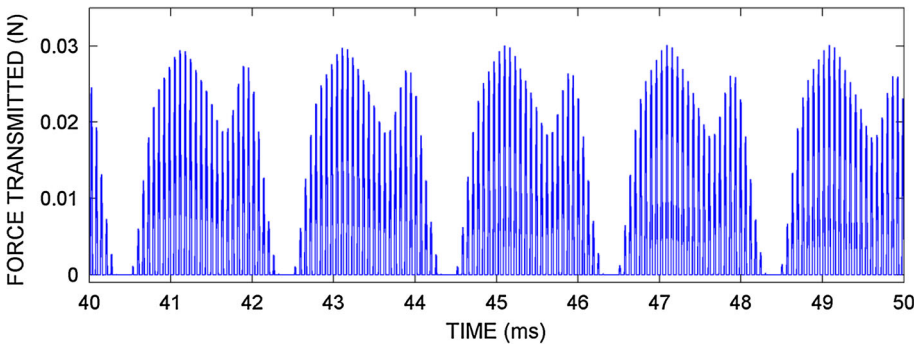

Fig. 17 Numerical simulation of transmitted force corresponding to breather propagation in the single chain with excitation amplitude $A = 11.66\,\mu$m and frequency 500 Hz; note the silent regions between the transmitted oscillatory wavepackets

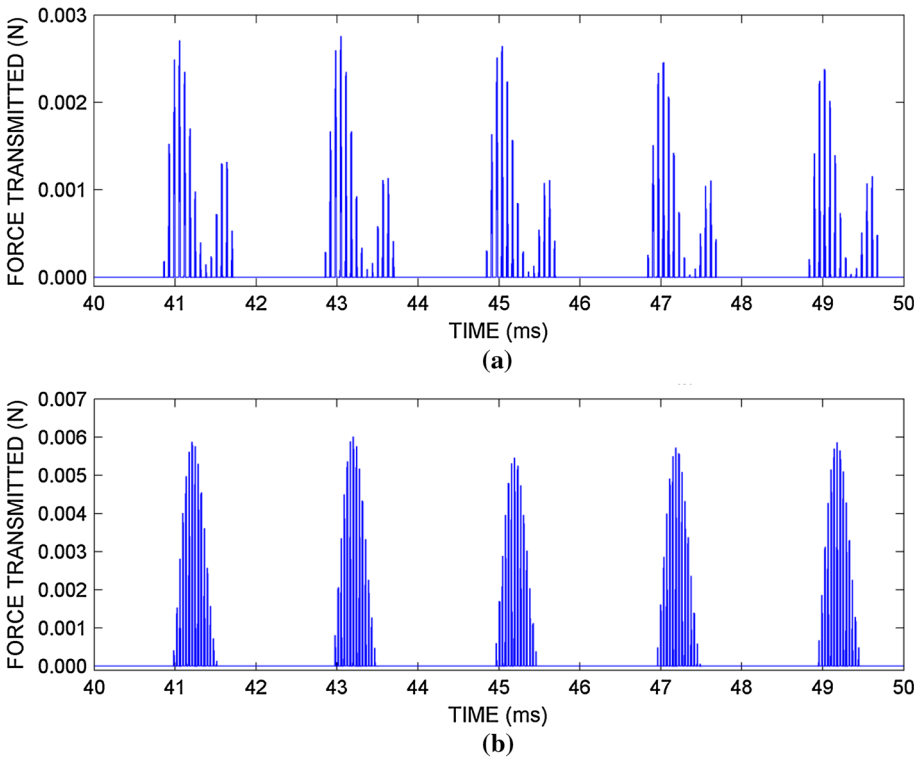

Fig. 18 Numerical simulation of transmitted force for breather propagation in the single chain at 500 Hz with (**a**) excitation amplitude $A = 7.0 \times 10^{-6}$m and coefficient of elastic foundation $k_1 = 3.16 \times 10^7$N/m, and (**b**) $A = 46.65 \times 10^{-6}$m and $k_1 = 9.48 \times 10^7$ N/m; note the variability of the waveforms of the localized wavepackets and the silent zones between them

In Fig. 17 we depict the time series of transmitted force at the right boundary of a single chain with parameters $m = 0.0036$ Kg, $k_1 = 3.16 \times 10^7$ N/m, $\gamma = 1.05 \times 10^6$ N/m, $\lambda_{k_1} = 0.78$ Ns/m, $\lambda_1 = 0.29$ Ns/m, $k_2 = \lambda_{k_2} = 0$, and $\delta_0 = 0.05 \times 10^{-6}$ m, forced by a harmonic base excitation with amplitude $A = 11.66 \times 10^{-6}$ m and frequency 500 Hz. The realization of a propagating localized wave packet (breather) is clearly evident from these results. Moreover, silent zones between wavepackets are noted, which can be tuned depending on the excitation amplitude, the foundation stiffness and the static pre-compression. This is demonstrated by the results of Fig. 18 where the waveforms of, and silent zones between, the propagating wavepackets at excitation frequency of 500 Hz have been changed by varying the stiffness coefficient k_1 of the elastic foundation and the amplitude of the applied excitation A. These numerical results are qualitatively similar to the experimental results presented in Fig. 8 for the single chain embedded in PDMS matrix, which demonstrates the capacity of the simplified model (1) to qualitatively capture the breather dynamics in the intermediate frequency range.

Similar results were obtained for systems with coupled chains when the experimentally measured propagating breather responses were numerically reconstructed. In addition, the model can help in the study of nonlinear energy transfers between the excited and absorbing chains and for predictive design of this acoustic metamaterial for prescribed energy exchanges [18]. In the numerical simulations we have taken into consideration the two remaining coupling parameters k_2, and λ_{k_2}, and prescribed harmonic base motion of the first bead of the excited chain with driving frequency 500 Hz and varying excitation amplitude.

In Fig. 19 we depict the transmitted force at the right boundary of the absorbing chain and the velocity of the

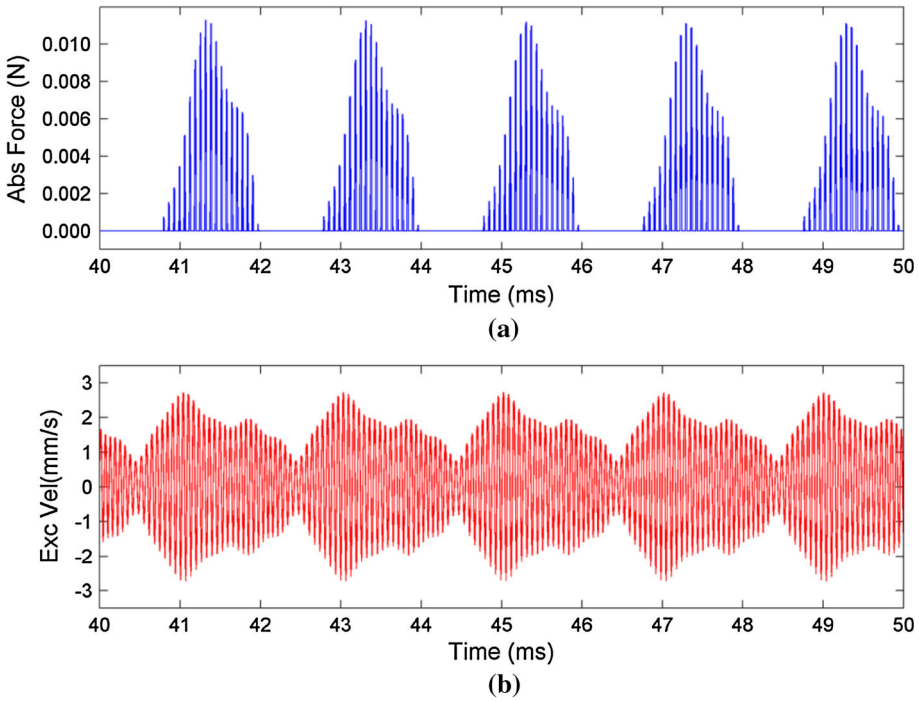

Fig. 19 Numerical simulation of transmitted force for breather propagation in the coupled chain with 0.5 mm lateral gap at 500 Hz and excitation amplitude $A = 11.66 \times 10^{-6}$ m; transmitted force at the right boundary of the absorbing chain (*top*), and velocity of the last granule of the excited chain (*bottom*)

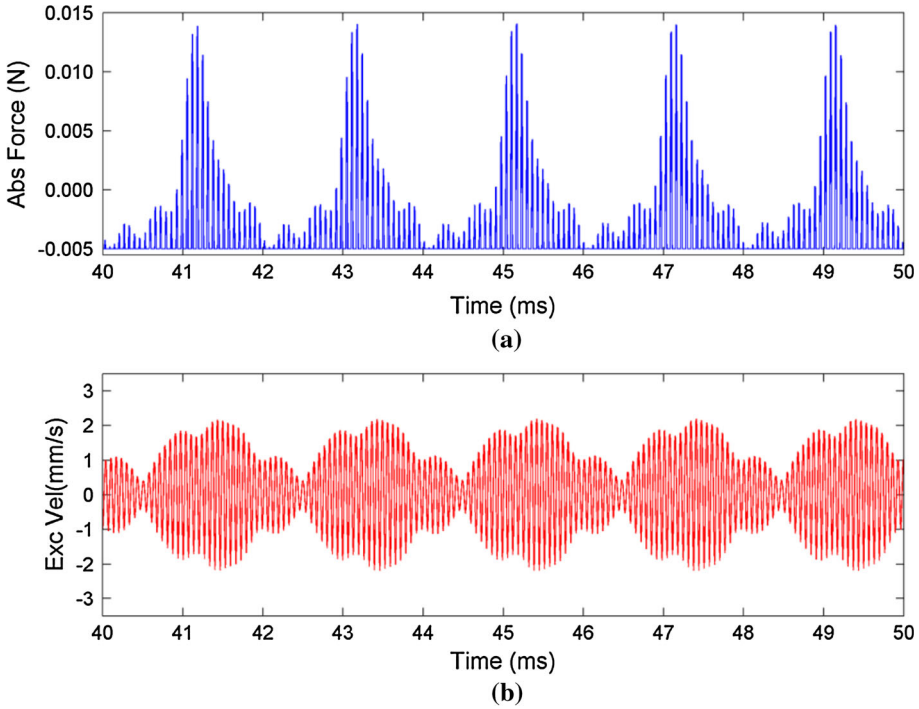

Fig. 20 Numerical simulation demonstrating the persistence of the propagating breather in the coupled chain with 10 times stronger coupling stiffness between the chains compared to the system considered in Fig. 19; transmitted force at the right boundary of the absorbing chain (*top*), and velocity of the last granule of the excited chain (*bottom*)

last granule of the excited chain for a coupled chain with normalized parameters $k_1 = 3.16 \times 10^7$ N/m, $\gamma = 1.05 \times 10^6$ N/m, $\lambda_{k_1} = 0.78$ Ns/m, $\lambda_1 = 0.29$ Ns/m, $\delta_0 = 0.05 \times 10^{-6}$ m, $k_2 = 7.42 \times 10^4$ N/m, $\lambda_{k_2} = 1.4$ Ns/m, with excitation amplitude $A = 11.66 \times 10^{-6}$ m and frequency 500 Hz; according to the identification performed in [18] these coupling parameters correspond to 0.5 mm lateral gap between chains embedded in PDMS matrix. The numerical results are qualitatively similar to the experimental results presented in Fig. 9a, and show clearly the formation of the propagating breather in this system, and the resulting intense nonlinear energy exchanges between the excited and absorbing chains.

By increasing the coupling stiffness parameter k_2 we induce stronger coupling between the two chains (as in the cases of granular chains embedded in polyurethane or geopolymer matrices), and affect the waveforms of the prop-

agating localized wavepackets. In Fig. 20 we present numerical simulations for a coupling stiffness parameter 10 times higher than the one used in the simulation of Fig. 19 (and identified in [18]), and with the other parameters kept fixed. From these simulations we deduce the persistence of the propagating breather in the system with stronger coupling and the corresponding intensification of the nonlinear energy exchanges between the granular chains.

These numerical simulations demonstrate the capacity of the simplified models of Fig. 16 to reproduce qualitatively the propagating breathers in single and coupled embedded granular chains. Similar results (not reported here) were obtained for the pass and stop-band dynamics of the experimental systems, indicating that these simplifying models can be used in a predictive capacity when designing granular metamaterials with prescribed properties and energy exchanges between the chains. This effort can be achieved by systematic identification of parameter properties of the experimental fixtures adopting optimization procedures similar to those developed in [18], followed by parametric studies for determining optimal material system designs.

4 Concluding remarks

In this work we experimentally studied the acoustic pass- and stop-bands, and the formation of propagating breathers in harmonically excited single or coupled ordered granular chains of steel beads embedded in three different types of matrix, namely PDMS, polyurethane and geopolymer. In agreement with theoretical predictions in previous works we confirmed the strongly nonlinear pulse-like response of these highly discontinuous media in low-frequency pass-bands, and their almost linear attenuatory dynamics in high-frequency stop-bands. Thus, we experimentally demonstrated the high tunability of this class of acoustic metamaterials to frequency (and energy) and proved that their dynamics undergo significant qualitative changes with varying frequency. Moreover, we experimentally proved that propagating breathers are formed at intermediate frequency ranges, representing a strongly nonlinear intermediate state of the granular dynamics in the transition between pass-bands and stop-bands. The propagating breathers were robustly excited in both single and coupled chains and with matrices with drastically different stiffness and dissipative material properties. These motions are generated due to modulational instability and are formed by a dynamical balance of the nonlinear Hertzian interactions in the embedded granular chains, the on-site potential provided by the matrix and the discreteness of the medium. Simplified theoretical models of these highly complex acoustic metamaterials theoretically confirm the existence of discrete breather responses at intermediate frequency regimes.

The findings reported in this work have potential applications in the design of acoustic metamaterials incorporating intentional strong nonlinearity. These media can be applied as acoustic filters, i.e., as passive dissipaters of disturbances generated by shock and vibration at specific frequency and energy ranges. Moreover, the formation of propagating breathers in this class of strongly nonlinear metamaterials can find application in passive energy redirection designs. Indeed, as shown in [17], coupled granular chains that support propagating breathers can be designed for passive wave redirection by implementing spatial Landau–Zener tunneling. This effect, which was first studied in a quantum mechanical context, induces slow uni-directional transfer of energy between coupled dynamical systems in resonance when spatial stratification of the foundation stiffness results in gradual escape from the resonance state. As shown by Hasan et al. [17] who applied this concept in the context of coupled granular chains, Landau–Zener tunneling can be implemented also in space, by gradually stratifying the foundation stiffness of one chain so that propagating breathers initially propagating in both chains are passively and irreversibly redirected to a single chain (the receiver). Such designs can result in granular metamaterials with the capacity to passively redirect shock-induced disturbances to *a priori* determined paths, where they are localized and effectively dissipated locally. In general, the results of this work contribute to the design of practical nonlinear granular metamaterials that are tunable and adaptive to different types of external broadband or narrowband excitations.

Acknowledgments This work was funded by MURI grant US ARO W911NF-09-1-0436. Dr. David Stepp is the grant monitor.

References

1. Aubry, S.: Breathers in nonlinear lattices: existence, linear stability and quantization. Phys. D **103**, 201–250 (1997)
2. Bell, J.L., Driemeyer, P.E., Kriven, W.M.: Formation of ceramics from metakaolin-based geopolymers, part II: K-based geopolymer. J. Am. Ceram. Soc. **92**(3), 607–615 (2009)
3. Berman, G.P., Izrailev, F.M.: The Fermi–Pasta–Ulam problem: fifty years of progress. Chaos **15**(1), 015104 (2005)
4. Boechler, N., Daraio, C.: An experimental investigation of acoustic band gaps and localization in granular elastic chains. In: Proceedings of the 22nd ASME Biennial Conference on Mechanical Vibration and Noise, San Diego, CA (2009)
5. Boechler, N., Theocharis, G., Job, S., Kevrekidis, P.G., Porter, M.A., Daraio, C.: Discrete breathers in one-dimensional diatomic granular crystals. Phys. Rev. Lett. **104**(24), 244302 (2010)
6. Brunhuber, C., Mertens, F.G., Gaididei, Y.: Envelope solitons on anharmonic damped atomic chains. Phys. Rev. E **73**(1), 016614 (2006)
7. Coste, C., Falcon, E., Fauve, S.: Solitary waves in a chain of beads under Hertz contact. Phys. Rev. E **56**(5), 6104–6117 (1997)
8. Daraio, C., Nesterenko, V.F., Herbold, E.B., Jin, S.: Energy trapping and shock disintegration in a composite granular medium. Phys. Rev. Lett. **96**(5), 058002 (2006a)

9. Daraio, C., Nesterenko, V.F., Herbold, E.B., Jin, S.: Tunability of solitary wave properties in one-dimensional strongly nonlinear phononic crystals. Phys. Rev. E **73**(2), 026610 (2006b)
10. Dauxois, T., Peyrard, M.: Energy localization in nonlinear lattices. Phys. Rev. Lett. **70**(25), 3935–3938 (1993)
11. Dauxois, T., Khomeriki, R., Piazza, F., Ruffo, S.: The anti-FPU problem. Chaos **15**(1), 015110 (2005)
12. Duxsona, P., Provis, J.L., Lukey, G.C., Mallicoat, S.W., Kriven, W.M., van Deventer, J.S.J.: Understanding the relationship between geopolymer composition, microstructure and mechanical properties. Colloids Surf. A **269**, 47–58 (2005)
13. Engheta, N., Ziolkowski, R.W.: Metamaterials: Physics and Engineering Explorations. Wiley, New York (2006)
14. Flach, S., Willis, C.R.: Discrete breathers. Phys. Rep. **295**, 181–264 (1998)
15. Flach, S., Gorbach, A.V.: Discrete breathers—advances in theory and applications. Phys. Rep. **467**(1–3), 1–116 (2008)
16. Hasegawa, A.: Generation of a train of soliton pulses by induced modulational instability in optical fibers. Opt. Lett. **9**(7), 288–290 (1984)
17. Hasan, M.A., Starosvetsky, Y., Vakakis, A.F., Manevitch, L.I.: Nonlinear targeted energy transfer and macroscopic analog of the quantum Landau–Zener effect in coupled granular chains. Phys. D **252**, 46–58 (2013a)
18. Hasan, M.A., Cho, S., Remick, K., Vakakis, A.F., McFarland, D.M., Kriven, W.M.: Primary pulse transmission in coupled steel granular chains embedded in PDMS matrix: experiment and modeling. Int. J. Solids Struct. **50**(20–21), 3207–3224 (2013b)
19. Hladky-Hennion, A.-C., Allan, G., de Billy, M.: Localized modes in a one-dimensional diatomic chain of coupled spheres. J. Appl. Phys. **98**(5), 054909–054909-7 (2005)
20. Hladky-Hennion, A.-C., de Billy, M.: Experimental validation of band gaps and localization in a one-dimensional diatomic phononic crystal. J. Acoust. Soc. Am. **122**(5), 2594–2600 (2007)
21. James, G.: Nonlinear waves in Newton's cradle and the discrete p-Schrödinger equation. Math. Models Methods Appl. Sci. **21**, 2335–2377 (2011)
22. James, G., Kevrekidis, P.G., Cuevas, J.: Breathers in oscillator chains with Hertzian interactions. Phys. D **251**, 39–59 (2013)
23. Jayaprakash, K.R., Starosvetsky, Y., Vakakis, A.F., Peeters, M., Kerschen, G.: Nonlinear normal modes and band zones in granular chains with no pre-compression. Nonlinear Dyn. **63**(3), 359–385 (2011)
24. Kriven, W.M.: Inorganic polysialates or 'geopolymers. Am. Ceram. Soc. Bull. **89**(4), 31–34 (2010)
25. Lazaridi, A.N., Nesterenko, V.F.: Observation of a new type of solitary waves in a one-dimensional granular medium. J. Appl. Mech. Tech. Phys. **26**(3), 405–408 (1985)
26. Lydon, J., Jayaprakash, K.R., Ngo, D., Starosvetsky, Y., Vakakis, A.F., Daraio, C.: Frequency bands of strongly nonlinear homogeneous granular systems. Phys. Rev. E **88**(1), 012206 (2013)
27. MacKay, R.: Solitary waves in a chain of beads under Hertz contact. Phys. Lett. A **251**(3), 191–192 (1999)
28. Marquie, P., Bilbault, J.M., Remoissenet, M.: Generation of envelope and hole solitons in an experimental transmission line. Phys. Rev. E **49**(1), 828–835 (1994)
29. Martínez, P.J., Meister, M., Floría, L.M., Falo, F.: Dissipative discrete breathers: periodic, quasiperiodic, chaotic, and mobile. Chaos **13**(2), 610–623 (2003)
30. Martinsson, P.G., Movchan, A.B.: Vibrations of lattice structures and phononic band gaps. Q. J. Mech. Appl. Math. **56**(1), 45–64 (2003)
31. Nesterenko, V.F.: Propagation of nonlinear compression pulses in granular media. J. Appl. Mech. Tech. Phys. **24**(5), 733–743 (1983)
32. Nesterenko, V.: Dynamics of Heterogeneous Materials. Springer, Berlin (2001)
33. Sen, S., Hong, J., Bang, J., Avalos, E., Doney, R.: Solitary waves in the granular chain. Phys. Rep. **462**(2), 21–66 (2008)
34. Sen, S., Mohan, T.R.K.: Dynamics of metastable breathers in nonlinear chains in acoustic vacuum. Phys. Rev. E **79**(3), 036603 (2009)
35. Shamonina, E., Solymar, L.: Metamaterials: how the subject started. Metamaterials **1**(1), 12–18 (2007)
36. Starosvetsky, Y., Vakakis, A.F.: Traveling waves and localized modes in one-dimensional homogeneous granular chains with no precompression. Phys. Rev. E **82**(2), 026603 (2010)
37. Starosvetsky, Y., Jayaprakash, K.R., Vakakis, A.F.: Scattering of solitary waves and excitation of transient breathers in granular media by light intruders and no precompression. J. Appl. Mech. **79**(1), 011001–011001 (2011)
38. Starosvetsky, Y., Hasan, M.A., Vakakis, A.F., Manevitch, L.I.: Strongly nonlinear beat phenomena and energy exchanges in weakly coupled granular chains on elastic foundations. SIAM J. Appl. Math. **72**(1), 337–361 (2012)
39. Starosvetsky, Y., Hasan, M.A., Vakakis, A.F.: Nonlinear pulse equipartition in weakly coupled ordered granular chains with no precompression. J. Comput. Nonlinear Dyn. **8**(3), 034504–034504 (2013)
40. Szelengowicz, I., Hasan, M.A., Starosvetsky, Y., Vakakis, A., Daraio, C.: Energy equipartition in two-dimensional granular systems with spherical intruders. Phys. Rev. E **87**(3), 032204 (2013)
41. Theocharis, G., Kavousanakis, M., Kevrekidis, P.G., Daraio, C., Porter, M.A., Kevrekidis, I.G.: Localized breathing modes in granular crystals with defects. Phys. Rev. E **80**(6), 066601 (2009)
42. Theocharis, G., Boechler, N., Kevrekidis, P.G., Job, S., Porter, M.A., Daraio, C.: Intrinsic energy localization through discrete gap breathers in one-dimensional diatomic granular crystals. Phys. Rev. E **82**(5), 056604 (2010)